C.P. No. 537

C.P. No. 537

MINISTRY OF AVIATION

AERONAUTICAL RESEARCH COUNCIL

CURRENT PAPERS

Flow Fluctuations and Alternating Blade Stresses in a Single-stage Compressor; a comparison with Multi-stage Tests

By

By R. Chaplin

LONDON: HER MAJESTY'S STATIONERY OFFICE

1961

PRICE 7s 6d NET

U.D.C. No. 621.438.031.3-226.2:
539.3:621.004.63

C.P. No. 537

April, 1958

Flow fluctuations and alternating blade stresses in a single-stage compressor; a comparison with multi-stage tests

- by -

R. Chaplin

SUMMARY

A single-stage compressor was assembled to be identical with the first stage of a multi-stage compressor. The fluctuations in axial velocity and the alternating stresses in the blades were measured and are compared with those which existed in the multi-stage compressor at identical speeds and non-dimensional flows.

No similarity was observed in the number, size or speed of rotation of the stall cells and it is concluded that measurements of alternating stress in a single-stage compressor are not necessarily a guide to those in the same stage when forming part of the multi-stage compressor.

Using a simplified and approximate method, the alternating blade stresses have been calculated from the observed fluctuations in velocity and a reasonable agreement between measured and calculated values obtained.

CONTENTS

TABLES

APPENDICES

ILLUSTRATIONS

1.0 Introduction

Aerodynamic excitation of blading in an axial compressor may be produced by buffeting[1] or rotating stall cells[2,3,4] and is usually confined to off-design speeds.

An earlier investigation into the flow fluctuations and rotor blade stresses in the first stage of a multi-stage compressor has been made. This present investigation was undertaken to examine the stall cell region in the first stage of that compressor when operating in a single-stage rig. The scope of the investigation was widened to include the determination of the variation of stall cell magnitude before and after the rotor row and the measurement of the alternating stresses in the inlet guide vanes and stator blades.

2.0 Apparatus

2.1 Plant

The single-stage compressor rig is illustrated in Figure 1. The drive is taken through a step-up gear-box from a variable speed induction motor having a rated horse power of 1450 at 1485 rev/min. A liquid regulator is used for variation of speed; water cooling of this regulator allows the speed of the compressor to be controlled to ±20 rev/min. The arrangement of the working section is shown in Figure 2, the blades used being identical with those of the first stage of the compressor used in the previous test. Mechanical details of the blading are given in Table II.

Recordings were made of the mass flow, temperature rise and pressure ratios, the characteristics as measured are plotted in Figure 4; this figure also shows the range of V_a/U covered in the multi-stage compressor tests.

2.2 Instrumentation

Alternating stress

Wire strain gauges were attached to six inlet guide vanes, four rotor blades and six stator blades. The gauges were attached to the blades at the centre of the convex surface just above the root fillet. The four gauged rotor blades were on adjacent blades in pairs at 180° spacing around the wheel and were connected through slip rings to the gauge supply and selection panels. The gauged inlet guide and stator blades were also at equi-angular spacing and those stationary blades on which stress levels were recorded are indicated in Figure 2. The alternating stress level in the blades was displayed continuously throughout the tests for visual reference.

Flow fluctuations

The perturbations of axial velocity were measured by six hot wire anemometers in the positions shown in Figure 2, and the calculations performed by the method described in Appendix II. A section of the anemometer head and the supply and balancing network are shown in Figure 3. These anemometers were identical with those previously employed except for an improved radial traversing gear.

2.3 Recording and amplifying equipment

The recording equipment consisted of a six-channel oscillograph with a 70 mm camera, the film speed used was approximately 20 in/sec. The recording time was controlled by a simple condenser-resistance network to give an exposure of about 1 second excluding the time required for the film to reach a constant speed. (The output from a crystal controlled oscillator was frequency divided by a Decatron to provide 500 c/sec time marks.) Engine speed was obtained from a standard tacho-generator driven off an auxiliary shaft on the main gear-box; the output from the generator was passed through a shaping circuit to give well defined pulses and improve the accuracy of measurement. The time marking and revolution counting signals were applied to the opposite plates of the same cathode ray tube; signal senses were so arranged as to deflect the beam in opposite directions.

The strain gauges were wired to switch panels, arranged that any three gauges could be connected through amplifiers to the recorder. The gauges were energised from batteries of mercury cells to ensure uniformity of applied voltages over long periods of running.

Four amplifying channels were available for use with the hot wire anemometers. The frequency response of the amplifiers was adjusted to compensate for the finite time constant of the anemometers up to approximately 2000 c/sec. The response to velocity changes of frequencies below about 35 c/sec was affected by coupling impedances, and values of velocity changes quoted at frequencies less than this have been corrected for this effect.

3.0 Programme

It was considered that any periodic flow fluctuations in a blade row could be sufficiently defined with three anemometers, two at a known angle and the same radius to determine the speed of rotation and the magnitude at that radius, and a third at a different radius to fix the change in magnitude with radius. As the number of channels was limited it was necessary to make a minimum of four exposures at each condition of the compressor. These exposures being as follows:-

(1) I.G.V. anemometers + I.G.V. strain gauges

(2) I.G.V. anemometers + rotor blade strain gauges

(3) Stator anemometers + rotor blade strain gauges

(4) Stator anemometers + stator blade strain gauges

In this way it was possible to photograph the stress in two blades of each row simultaneously with the output from the anemometers either in the row or, in the case of the rotor blades, both before and after the blade row. In addition, recordings were taken to determine the relation between the flow fluctuations before and after the rotor row. The sixth channel was used for recording engine speed and time marks.

It was planned to survey, over a wide range of V_a/U, those speeds at which stall cells had been found in the multi-stage compressor. Accordingly records were made on constant speed characteristics over the full range of the throttle. These characteristics were taken at speed

intervals of 500 rev/min from 4000 rev/min to 5500 rev/min. The investigation was terminated by the failure of a rotor blade at 5500 rev/min after recordings at this speed had been completed.

4.0 Results

Characteristics were taken at 500 rev/min intervals from 4000 to 5500 rev/min, recordings being made at six values of V_a/U on each characteristic; these points are shown in Figure 4.

The measured values of alternating stresses in the fundamental flexural mode are plotted for all rows on Figures 5 to 9. As stated in Section 3.0 more than one recording was made of the alternating stress in a particular row at each point. If different values of the stress in a particular blade were obtained, these have been shown in the graphs. The alternating stresses in modes other than the fundamental are shown in Table III if greater than 0.5 tons/sq.in. Values of the perturbation level, stall cell numbers and rotational speeds are given in Table IV.

The alternating stresses in the inlet guide vanes were low throughout (Figure 5) and little attention is given to this row in the text. Detailed descriptions of the alternating stress and flow disturbances for each characteristic are given below.

4.1 4000 rev/min

The alternating blade stress and the perturbations in axial velocity were small and sporadic between $V_a/U = 0.55$ and 0.51 i.e. at flows greater than that of peak pressure rise. At $V_a/U = 0.51$ there was an increase in the perturbation level towards the inner diameter. Trace d of record A3/17 (shown in Figure 11) is the output from an anemometer located at 0.25 rotor blade height, indicating a perturbation level of ±2 per cent of mean V_a. The fluctuation is fairly regular and has a major component at shaft rotational speed.

At $V_a/U = 0.465$ there was a single stall cell rotating at approximately 29 per cent of rotational speed, the velocity change at 0.8 rotor blade height was about 50 per cent (peak to peak) of mean V_a. The cell is shown in the extract from record A4/19 (Figure 11) to have been entirely confined to the outer annulus as no trace of the disturbance is visible at mean diameter. The rotor blade stress increased at this point as shown in Figure 6; the influence of the stall cell on the alternating stress pattern can be seen in the extract.

After some ten minutes operation at this condition there was a sudden change in the stall cell formation to that illustrated by record A4/22 (Figure 11) without any noticeable change in the steady state conditions. The second state is that of two unequal cells rotating at about 35 per cent rotor speed with a magnitude of 26 per cent (peak to peak) of mean V_a at 0.8 rotor blade height and of 9 per cent (peak to peak) at mean diameter. The increase in excitation frequency caused an increase in rotor blade alternating stress, marked by the heavy modulation shown in the record A4/22. No significant increase in either stator blade or inlet guide vane alternating stress was observed.

As the value of V_a/U was decreased by further throttling to 0.295 the stall cell formation reverted to a single cell rotating at 28 per cent rotor speed, the magnitude at 0.8 rotor blade being approximately

50 per cent as for the single cell state at $V_a/U = 0.465$ but with considerably greater circumferential width and greater radial penetration (10 per cent at mean diameter). An extract from one of the records taken at this speed is in Figure 17. The rotor blade stress levels were similar to those for $V_a/U = 0.465$ but the stator blades showed an increase in alternating stress due to the rise in the mean diameter perturbation level.

The throttle was gradually closed until V_a/U fell to 0.18, and the throttling was accompanied by a gradual change from regular stall cells to random fluctuations. The fluctuations were larger at mean diameter than at 0.8 rotor blade height and there was a significant difference between perturbation level in the stator and in the inlet guide rows. The high perturbation level (17 per cent) at mean diameter in the stator row accounts for the further rise in the alternating stress in this row.

4.2 4500 rev/min

The stress levels and flow fluctuations followed the pattern encountered on the 4000 rev/min characteristic. For values of V_a/U (mean) of 0.49 and above, the perturbation levels were small <1.5 per cent at all diameters and the alternating stresses were also low. Record B3/52 on Figure 12 is typical of records in this region.

At $V_a/U = 0.45$ two stall cells rotating at between 34 and 36 per cent rotor speed were present, the velocity change within the cell at 0.8 rotor blade height amounting to 8 per cent and 21 per cent of mean V_a in the inlet guide and stator blade passages respectively. Extracts from records B4/60 and B4/63 are shown in Figure 12 to illustrate the stall cell form at this condition. Record B4/60 is of the output from the three anemometers in the inlet guide vane row and of the alternating stresses in two of the inlet guides. Record B4/63 is of the output of the three stator row anemometers and of the alternating stresses in two of the stator blades. A comparison of the two records shows that the velocity changes in the inlet guide row were almost sinusoidal compared with the marked saw tooth wave form in the stator row. It is also evident from the traces on B4/63 that there was no radial similarity in the velocity change at this point since the mean diameter trace shows a reversal of slope to the traces taken at 0.8 rotor blade height. The extracts indicate that the stator blades and the inlet guide vanes were vibrating in resonance with the second and third harmonics respectively of the stall cells, but the stresses were small since the cells were located at the roots of these blades. In record B4/60 the inlet guide vanes show a constant level of fairly high frequency stress. This frequency is that of rotor blade passage and coincides at this speed with that of the fourth flexural mode of vibration. The stress level at the blade root in this mode was about 0.5 tons/sq.in. at $V_a/U = 0.54$ and decreased slightly with decreasing values of V_a/U. A record of the alternating stress pattern in the rotor blades is included in Figure 13 to show the very short bursts of vibration occurring in these blades at this point.

As the throttle was closed to $V_a/U = 0.27$ the two cell state gave way to a single cell rotating at a speed of between 27 and 29 per cent of rotor speed. The magnitude of the velocity change at 0.8 rotor blade height was approximately 48 per cent both before and after the rotor row, but there was a greater radial penetration in the stator than in the inlet guides, the mean diameter figures being 8 and 13 per cent respectively. The wave form of the velocity change at this condition was ragged particularly in the stator row; this point is brought out by record B5/68

(Figure 13) which shows the velocity change recorded by anemometers at the same radius in both inlet guide and stator rows and in approximate axial alignment. Included in record B5/68 are the alternating stress patterns of single blades in each of the three rows. The influence of the stall cell is easily seen in the stress wave form of the inlet guide and to a lesser extent in the wave forms of the stator and rotor blades. The level of alternating stress in stator and rotor rows was approximately the same and was unchanged from that at $V_a/U = 0.45$ (Figures 6 and 8). The fall in excitation frequency being compensated by the increase in magnitude of the perturbations in axial velocity.

Random pulsations in axial velocity were again encountered at $V_a/U = 0.18$; again the fluctuation level was greater at mean diameter than towards the outer diameter and greater in the stator than in the inlet guide row. The fall in rotor blade vibratory stress at this point was due to the fall in perturbation level towards the rotor tip; the fall in rotor blade stress was accompanied by a rise in that of the stators owing to the increase in perturbation level at mean diameter. Figure 13 contains an extract from record B6/74 showing an anemometer in each stationary row and the alternating stress in each of the three rows.

4.3 5000 rev/min

Stall cells were encountered at the same throttle setting as on the previous characteristics, i.e. a little beyond the point of peak pressure rise. Recordings made at $V_a/U = 0.44$ showed the presence of two cells rotating at 35 per cent of rotational speed. The velocity change within the cell amounted to 11 per cent in the inlet guide row and to 28 per cent in the stator row at 0.8 rotor blade height. At this condition the cells were of variable width as can be seen in the extract from record C4/99 (Figure 14). This record contains the traces from the inlet guide anemometers and the alternating stresses in two of the rotor blades; the alternating stresses in the two rotor blades are shown to have risen and fallen simultaneously. Two cells rotating at 35 per cent rotor speed give a forcing frequency on the rotor blades of 106.5 c/sec with a second harmonic of 217 c/sec which is close to the natural frequency of the rotor blades at this speed. The frequency of vibration of the rotor blades (record C4/99) was approximately 222 c/sec and, considering the accuracy of the calculation of cell rotational speed, it is reasonable to assume that the rotor blades were being forced by the second harmonic of the stall cell formation. Figure 7 shows the increase of alternating stress in the rotor blades at this point.

The rotational speed of the stall cells fell to 31.2 per cent of rotor speed when V_a/U was reduced to 0.31, and the velocity change within the cell at 0.8 rotor blade height increased to 33 and 38 per cent in the inlet guide and stator rows respectively. The fall in rotational speed increased the excitation frequency on the rotor blades to 114.5 and 229 c/sec for the fundamental and second harmonics respectively. The latter frequency coincides with the calculated natural frequency at this speed (230 c/sec) and with the rise in excitation level accounts for the peak rotor blade stress shown in Figure 7; the resonance is illustrated in Figure 14 by an extract from record C5/105. The simultaneous recording of the alternating stresses in single blades of each row and the velocity changes in the inlet guide row (record C5/104 Figure 14) shows that at this point the stator blades and the inlet guide vane were being forced by the second and third harmonics respectively.

The two cell formations continued to exist as the throttle was closed, finally breaking down into random fluctuations as V_a/U approached 0.18. At this value of V_a/U the perturbations were large, averaging about 11 per cent of mean axial velocity, in both stator and guide vane rows.

4.4 5500 rev/min

The general pattern of events on this characteristic was identical with that found on the previous characteristic. Small perturbations in axial velocity with small alternating stresses in the blading were found at flows above that for $V_a/U = 0.45$. The two cell formation was established at $V_a/U = 0.43$ and persisted below $V_a/U = 0.29$. The rotational speeds were 32 and 31 per cent respectively. Random fluctuations were again observed at $V_a/U = 0.18$. The perturbation magnitudes given in Table IV are slightly smaller than for comparable conditions at 5000 rev/min.

In the stall cell region the excitation frequencies at this speed were above the natural rotor blade frequency and a reduced alternating stress was observed. The frequency of vibration of the rotor blades was that of the second harmonic of the stall cell frequency.

Three extracts from the records taken at 5500 rev/min form Figure 5. The extract from record D4/145 taken at $V_a/U = 0.43$ shows the alternating stress in a blade in each row and the velocity changes recorded by anemometers numbers 1 and 4 (Figure 2). Records D5/154 and D6/161 are of the same blades and anemometers at $V_a/U = 0.29$ and $V_a/U = 0.18$ respectively. The anemometer traces show the increase in annular width of the cell at $V_a/U = 0.29$ and the random perturbations at $V_a/U = 0.18$. The relatively pure fundamental flexural vibration of the rotor blade (upper trace) at $V_a/U = 0.43$ is replaced by vibration in the second flexural mode at $V_a/U = 0.18$. The alternating stress in the inlet guide vane was very small and is shown in the extracts to have been complex.

An enlargement of record D5/150 is on Figure 16; this extract has the traces from the four anemometers at 0.8 rotor blade height i.e. numbers 1, 3, 4 and 6. Anemometers numbers 1 and 4 subtend an angle of 5° at the axis and numbers 3 and 6 an angle of 15°. The measured delay at anemometer 1 relative to anemometer 4 and at anemometer 6 relative to anemometer 3 are in proportion to the above angles and the rotational speed of the cells indicating that there was little displacement between velocity peaks in the inlet guide and stator row.

5.0 Harmonic analysis of stall cell wave forms

To calculate the blade stress due to changes in air velocity it is necessary to know the frequency distribution of the velocity changes and it was intended, after the first survey of the stall cell region, to make harmonic analyses of the anemometer and strain gauge signals. This was prevented by a rotor blade failure and recourse was made to a planimetric method using enlargements of the oscillograph records.

The electrical harmonic analyser provides average values of the components of a particular wave form over a large number of cycles; this property is an advantage where the wave form is variable. The planimetric methods are used for the analysis of single cycles and are impracticable for obtaining average values. For this reason the values of the harmonic

components given in Table V may be unreliable for conditions at which the wave shape was erratic, for example that of the velocity changes in the single stall cell state at $V_a/U = 0.28$ on the 4000 and 4500 rev/min characteristics.

The method used was that of Daniels as developed by Crease and Tucker[5]. For a wave form in which the amplitude of a harmonic diminishes rapidly with order, the method requires only two area measurements to determine the amplitude of a particular harmonic.

In some cases fair agreement between recorded and "built up" wave forms was obtained after estimation of the first three harmonics. In other cases considerable discrepancy remained after the first five harmonics had been measured; the accuracy of the reproduction of the recorded wave shape did not justify estimation of further harmonics. Typical examples of enlarged recorded wave forms and "built up" wave forms are shown in Figure 10.

When the stall cell formation consisted of unequal cells or cells at unequal spacing such as at $V_a/U = 0.45$ at 4000 and 4500 rev/min, fractional orders were present. A simplified summary of the harmonic content of the stall cell formations is given below (non integral orders neglected).

Harmonic order	1	2	3	4
Amplitude range	50 - 90%	15 - 50%	5 - 40%	5 - 30%

6.0 Comparison of experimental and calculated alternating stresses in the rotor and stator blades

6.1 Method of calculation

In Appendix III it is suggested that a simple relation exists between the alternating blade stress and the fluctuations in fluid velocity. An approximate equation, given below, is derived and shown to apply to the first-stage rotor blades of a multi-stage compressor.

$$\frac{\Delta q}{q} = \frac{\Delta v}{v} \cdot Q' \cdot (W.F.) \cdot \left(1 - \frac{PU^2}{Kp\Delta T}\right)$$

in which $\bar{q}$ = blade stress (mean gas bending)

Δq = fluctuation in blade stress

$\bar{v}$ = mean axial velocity

Δv = perturbation in axial velocity

Q' = dynamic amplification factor

W.F. = perturbation distribution factor

$$P = \frac{d(\tan \alpha_1 - \tan \alpha_2)}{d(\tan \alpha_1)}$$

U = rotational speed (mean diameter)

Kp = specific heat (constant pressure)

ΔT = stage temperature rise

The perturbations in axial velocity cover a wide frequency range and produce on the blades forces of a similar spectrum. The alternating stress produced by a force of a particular frequency depends on the difference between that frequency and that of the mode of vibration being considered, and on the logarithmic decrement in that mode. It is more convenient to use the dynamic amplifcation factor $\zeta = \frac{\pi}{\log dec}$ as it allows the use of the universal response curve[6] associated with resonance in electrical circuits. From such a curve, the dynamic amplifier Q' for a component of frequency f can be read.

As stated in Appendix III, a ζ of 10 was found experimentally for a blade of the same size, material and characteristics as the rotor blades used in this compressor, and a Q of 16 for the same blade in aluminium bronze. These ζ factors have been used for the rotor and stator blades in the calculations.

The velocity change in the stall cell may vary along the blade length; in this case the fluctuations were greatest at the rotor tips and were small at mean diameter. The derivation of the blade stress assumes a uniform axial velocity along the blade and the perturbation distribution factor was introduced to convert the observed distribution into a uniform distribution with the same bending moment at the root.

For the rotor blades a parabolic distribution was assumed. Such a distribution having an observed magnitude h at 0.8 rotor blade height has approximately the same bending moment as a uniform load of 0.83 h.

The stator blades are not sensitive to the velocity changes at the outer diameter but are sensitive to changes at mean diameter. A triangular distribution was used, defined by taking the average velocity change at mean diameter to be one-third that at 0.8 rotor blade height. With this assumption, the equivalent uniform load is one of approximately 0.22 h.

The remaining factor P was taken as 2 throughout, i.e. the vector mean angle was unchanged.

The alternating stresses in the rotor and stator blades were calculated as above using those harmonics of the stall cells with frequencies close to the natural frequency of the blades. The higher assumed ζ of the stator blades reduced the number of harmonics to be considered in the calculation of the stresses in these blades. The calculations have not been extended to the region of random flow ($V_a/U \leq 0.25$ and $V_a/U \geq 0.48$) because of the difficulty and inaccuracy of "manual" analysis of random wave forms.

The range of the maximum observed alternating stress in the blading and, for comparison, the calculated stress due to the components of the stall cells are shown in Table VI. The total calculated stress depends on the relative phases of the components but where the stall cell outline is irregular it is reasonable to assume that at some time the components will be additive. At the resonance point (5000 rev/min $V_a/U = 0.3$) the stall cells were regular and an estimate of the phase difference of the first and second harmonics has been made; the figure given in the total column for this point is phase corrected.

6.2 Comparison of observed and calculated stress values

The measured alternating stress figures listed in Table VI are the maximum values found during a one second exposure, whereas the calculated values are those obtained using the harmonic content figures extracted from a particular stall cell cycle. For this reason the accuracy obtained should vary with the stability of the cells. The agreement of the measured and calculated values of rotor blade alternating stress is however good except at the point $V_a/U = 0.46$ on the 4000 rev/min characteristic where the stall cell formation consisted of two unequal cells. At this point the calculated maximum stress is only 70 per cent of the observed maximum stress.

The agreement of calculated and observed stator blade stress is reasonable except at points of $V_a/U = 0.46$ and 0.29 on the 4000 rev/min characteristic where the calculated values are much lower than those measured.

The locations of the anemometers were at mean diameter and towards rotor blade tip and no radial traverses were undertaken in these conditions. Hence there may have been unobserved fluctuations at the inner diameter which would account for the increased stator blade stress.

7.0 Comparison of the results of the single and multi-stage tests

One of the main objects of this test was to compare the stall cell region in a single-stage compressor with that existing in the same stage when forming the first stage of a multi-stage compressor. The flow in the stall cell region in the single stage has been described in Section 4.0 and is summarized below:-

(i) At flows above that of peak pressure rise ($V_a/U = 0.48$) the perturbations were small (c. 1 per cent of mean V_a) and irregular.

(ii) Between $V_a/U = 0.46$ and 0.25 stall cells were present rotating at between 28 and 35 per cent of rotor speed.

(iii) Below $V_a/U = 0.25$ large random fluctuations.

At 5000 and 5500 rev/min two cells were present over the range $V_a/U = 0.46$ to 0.25 and at 4000 and 4500 rev/min two cells at $V_a/U = 0.46$ merging to a single cell at about $V_a/U = 0.3$. The cells were confined to the outer annulus with little radial penetration beyond mean diameter, at 0.8 rotor blade height the average velocity change in the stator row was ±17 per cent of mean V_a.

In the multi-stage tests, characteristics were taken at 4000, 4500 and 5700 rev/min. At 4000 rev/min stall cells were encountered within the range $V_a/U = 0.35$ to $V_a/U = 0.26$, random perturbations occurring at values of $V_a/U \leq 0.25$. At 4500 rev/min, stall cells were present at all attainable values of V_a/U greater than the surge value, and at 5700 rev/min stall cells when V_a/U was decreased below $V_a/U = 0.36$. In the above region the only formation observed was that of three cells rotating at between 45 per cent and 50 per cent of rotor speed. Measured at the same radius as on the single-stage rig, the velocity changes averaged ±30 per cent of mean V_a. In Figure 17 and 18 are shown records taken on the single-stage and on the multi-stage compressor at approximately the same rotational speeds and values of V_a/U. These records have been adjusted to have the same time scales.

A comparison of the above shows that little similarity exists in the flow patterns in the two cases, and that even where stall cells are common to both, the number, size and rotational speed are different. This implies that stress levels measured on a single-stage rig are not necessarily a guide to those which would occur in the same stage when forming part of a multi-stage compressor. This is confirmed by the strain gauge recordings which show a resonance of the rotor blades with the second stall cell harmonic at 5000 rev/min and $V_a/U = 0.3$ yielding an alternating stress of ±5 tons; such a resonance could not occur in the multi-stage tests owing to the higher stall cell frequency.

8.0 Discussion

The type of stall which occurred on the single-stage compressor is known as progressive stall and is common to most axial compressors with a low ratio of internal to external diameters[8]. As the flow through such a stage is reduced, the blading stalls in patches depending on the local incidence. With further flow reduction the stalled patches increase in circumferential width and radial extent. Many incidences of progressive changes in the number of cells have been reported during this process. The changesin area of individual cells and changes in number result in a fairly uniform increase in stalled flow area and a gradual fall in the pressure ratio.

The behaviour of the single-stage compressor followed the general pattern above. The change in cell area with flow reduction can be clearly seen on Figure 15. The increase in area of the stalled flow and the increase in associated velocity change which took place in the stator row were accompanied by increased penetration upstream into the inlet guide vanes.

The single and multi-stage tests do not provide any positive information on the factors controlling the number of stall cells present at any particular condition. The single-stage tests show that over a wide range of V_a/U the number of cells can remain constant and that at a particular value of V_a/U the number of cells may be different for differing values of U. Similarly, a comparison of the single and multi-stage tests shows that, at identical speeds and flows, the number and speed of rotation of the cells are not the same. These results demonstrate that the mean flow coefficient of a stage does not control the number of cells. As it is the number and rotational speed of the stall cells which control the frequency of exciting forces on the blades, the alternating stresses measured in the single and multi-stage tests are not comparable.

The forces on the blades due to the presence of stall cells of irregular and variable outline is equivalent to a single frequency force at the mean stall cell frequency plus a general buffeting type of excitation at the blade natural frequency. Where the stall cells are uniform the transient vibration will be damped out and will not be observed. It is therefore possible to have beats between the natural and forced vibrations of the blades, the difference of the frequencies being the beat frequency[9]. This phenomenon is visible on record A4/22 (Figure 11), the natural frequency of the rotor blades at this speed was 217 c/sec and that of the two-and-a-half harmonic of the stall cells 233 c/sec. The difference frequency of 14 c/sec is equivalent to a beat length of approximately 15 cycles of the rotor blade vibration.

The successful application of the simple flow-stress relation over a wider flow range and for a different forcing spectrum to that found in the multi-stage tests is of considerable interest. If this relation is valid, then the effect of small changes in blade stiffness on the alternating stress on the blades can be determined. If recordings of the velocity fluctuations and alternating blade stresses in a particular compressor were made, then the alternating stresses in blades of stiffnesses differing from those of the blades employed may be calculated or deduced from electrically simulated blades. The range over which such a method can be used is limited. The change in blade shape required to effect the stiffness change must not materially affect the stall cell characteristics and the stiffness changes must not give rise to other forms of vibration.

9.0 Conclusions

The main conclusions to be drawn from these tests are:-

(1) The numbers of stall cells present in a stage are not governed by the mean flow coefficient.

(2) The alternating stresses in blades of a single-stage compressor are not necessarily a guide to those existing in the same stage when forming part of a multi-stage compressor.

(3) The relation between alternating stresses and changes in axial velocity in the stall cell region proposed in Appendix III has been shown to apply to the rotor and stator blades of this compressor.

ACKNOWLEDGMENTS

The author is indebted to Messrs. Metropolitan-Vickers Limited for placing at his disposal the Zephyr rig test facility, also to Dr. K. W. Todd and staff of the Gas Turbine Department and Mr. Roberts and staff of the Research Department of Messrs. Metropolitan-Vickers Limited for their help in these experiments and for supplying some of the data. The author is also grateful for the help and advice given by Mr. T. J. Hargest of N.G.T.E. both in carrying out the experiments and in the analysis of the results.

REFERENCES

No.	Author(s)	Title, etc.
1	A. D. S. Carter D. A. Kilpatrick C. E. Moss J. Ritchie	An experimental investigation of the blade vibratory stresses in a single-stage compressor. C.P. 266, June, 1955.
2	T. Iura W. D. Rannie	Experimental investigation of propagating stall in axial flow compressors. Trans. A.S.M.E. Vol. 76, No. 3, April, 1954.
3	Eleanor L. Costilow M. C. Huppert	Some effects of guide vane turning and stators on rotating stall characteristics of a high hub tip ratio single-stage compressor. N.A.C.A. TN.3711, 1956.
4	M. C. Huppert D. F. Johnson	Preliminary investigation of compressor blade vibration excited by rotating stall. N.A.C.A. RM.L52J15, 1953.
5	J. Crease M. J. Tucker	A note on an improved planimetric method of harmonic analysis. Brit. Journal Applied Physics, Vol. 5, No. 4, 1954.
6	F. E. Terman	Radio Engineering. McGraw Hill Book Co. Inc., 1937.
7	M. C. Huppert W. A. Benser	Some surge and stall phenomena in axial flow compressors. Journal Aero. Sciences, Vol. 20, No. 12, 1953.
8	S. Timoshenko	Vibration problems in engineering. D. Van Nostrand Co. Inc., 1937.
9	L. V. King	On the convection of heat from small cylinders. Phil. Trans. Roy. Soc. (A) Vol. 214, No. 14, pp. 373 and 432, 1914.
10	C. E. Pearson	Measurement of instantaneous vector air velocity by hot wire methods. J. Aero. Sci., Vol. 19, pp. 73 and 82, 1952.

REFERENCES (cont'd)

No.	Author(s)	Title, etc.
11	A. R. Howell	Design of axial flow compressors. Proc. Inst. Mech. E., Vol. 153, p. 455, 1945.

TABLE I

Test results

Test	Speed rev/min	V_a/U mean	Pressure ratio pitot	Pressure ratio static	Temp. rise °C
A	4000	0.554	1.053	1.053	5.6
A	"	0.528	1.056	1.056	5.8
A	"	0.504	1.057	1.058	6.2
A	"	0.463	1.056	1.051	7.5
A	"	0.292	1.041	1.036	12.6
A	"	0.180	1.042	1.046	10.5
B	4500	0.549	1.064	1.067	7.0
B	"	0.518	1.065	1.071	7.0
B	"	0.493	1.066	1.075	6.9
B	"	0.447	1.067	1.073	8.5
B	"	0.283	1.049	1.045	16.3
B	"	0.179	1.056	1.059	11.8
C	5000	0.528	1.085	1.081	7.8
C	"	0.509	1.087	1.085	7.6
C	"	0.488	1.090	1.091	8.5
C	"	0.440	1.084	1.076	8.8
C	"	0.302	1.074	1.060	17.2
C	"	0.181	1.089	1.069	16.1
D	5500	0.536	1.107	1.102	8.7
D	"	0.502	1.112	1.108	9.4
D	"	0.480	1.114	1.108	9.7
D	"	0.432	1.109	1.091	11.4
D	"	0.293	1.083	1.071	21.0
D	"	0.184	1.081	1.080	40.1

TABLE II

Blade details and frequencies

	Inlet guide vanes	Rotor blades	Stator blades
Material	Steel	Aluminium	Aℓ-Bronze
Aspect ratio	5.5	3.25	4.7
Number	96	38	56
Frequencies			
Fund. flexural	160 c/sec	190 c/sec	102 c/sec
Second flexural	570 "	770 "	530 "
Third flexural	1530 "	1890 "	1400 "
Fourth flexural	2804 "	3750 "	2777 "
Fifth flexural	4640 "	5470 "	4480 "
Sixth flexural	6684 "	7883 "	6444 "
Fund. torsional	1613	1157 "	1179
Second torsional	3341	2678 "	2901
Third torsional	5193	4419 "	4701
Fourth torsional	7245	6170 "	6645

The effect of centrifugal stiffening on the frequency of the fundamental flexural mode is given by:-

$$F_{(N)}^2 = F_o^2 + 2.4\,N^2$$

N = rev/sec

TABLE III

Blade stresses in the higher frequency modes of vibration

Test	Speed rev/min	V_a/U mean	Rotor blades				Stator blades			
A_5	4000	0.292	±0.5	tons/sq.in.	730	c/sec	±1.9	tons/sq.in.	530	c/sec
A_6	"	0.180	±0.9	"	"	"	±0.8	"	"	"
B_4	4500	0.447	±0.7	"	750	"	±0.9	"	535	"
B_5	"	0.283	±1.0	"	"	"	±1.5	"	"	"
B_6	"	0.179	±0.7	"	"	"	±0.8	"	"	"
C_4	5000	0.440	±0.5	"	760	"	±1.2	"	540	"
C_5	"	0.302	±0.5	"	"	"	±2.4	"	"	"
C_6	"	0.181	±1.25	"	"	"	±1.5	"	"	"
D_4	5500	0.432	± -				±1.6	"	542	"
D_5	"	0.293	±0.8	"	785	"	±3.2	"	"	"
D_6	"	0.184	±1.25	"	"	"	±2.5	"	"	"

At 4500 rev/min the inlet guide vanes showed an alternating stress of approximately ±0.5 tons at all points on the characteristic. The frequency of vibration was approximately 2800 c/sec.

TABLE IV

Magnitude and rotational speed of the fluctuations in axial velocity

Speed rev/min	V_a/U mean	No. of cells	Rotational speed	Average perturbation level (% V_a mean)			
				Inlet guide row		Stator row	
				0.8 rotor h	Mean dia.	0.8 rotor h	Mean dia.
4000	0.554	-	-	1.0%	-	-	1.5%
"	0.528	-	-	1.4%	-	1%	1.8%
"	0.504	-	-	1.2%	-	0.8%	-
"	0.463	1	29%	47%	-	-	-
"	0.463	2	35%	-	-	26%	9%
"	0.292	1	28%	48%	9%	50%	12%
"	0.181	-	-	6%	14%	11%	17%
4500	0.549	-	-	1.0%	-	1.2%	1.0%
"	0.518	-	-	1.1%	1.2%	0.7%	1.1%
"	0.493	-	-	1.2%	0.8%	1.0%	1.1%
"	0.447	2	35%	8.0%	4.0%	21%	4%
"	0.283	1	28%	46%	8.0%	50%	13%
"	0.179	-	-	6.0%	13%	11%	18%
5000	0.528	-	-	2.6%	4%	0.5%	1.0%
"	0.509	-	-	2.3%	3%	1.2%	1.2%
"	0.488	-	-	1.5%	2%	0.5%	1.0%
"	0.440	2	35%	11%	3%	28%	-
"	0.302	2	31.2%	34%	4%	38%	6%
"	0.181	-	-	11%	11%	12%	9%
5500	0.536	-	-	0.6%	0.6%	0.5%	0.6%
"	0.502	-	-	0.6%	0.6%	0.5%	0.5%
"	0.450	-	-	0.6%	0.7%	0.7%	0.7%
"	0.432	2	32%	10%	2.0%	24%	4%
"	0.293	2	31%	26%	3.0%	36%	5%
"	0.184	-	-	-	6%	-	11%

The perturbation level quoted is the average value of the peak to peak velocity change expressed as a percentage of the mean axial velocity.

TABLE V

Harmonic content of stall cell wave forms

Speed rev/min	V_a/U mean	Harmonic component of order							
		$\frac{1}{2}$	1	$1\frac{1}{2}$	2	$2\frac{1}{2}$	3	4	5
4000	0.463 (1)		85%		47%		23.5%	15%	15%
"	" (4)	23%	62%	39%	15%	22%			
"	0.292 (4)		52%		32%		41%	28%	18%
4500	0.447 (1)	21%	50%	25%	30%	23%			
"	0.283 (1)		90%		48%		27%	20%	17%
5000	0.302 (1)		92%		42%		7%	8.5%	
5500	0.432 (1)		90%		37%		17%	8%	
"	" (4)		76%		36%		13%	11%	
"	0.293 (1)		93%		33%		11%		
"	" (4)		74%		31%		21%	9%	

The wave form analysed was that from anemometers at 0.8 rotor blade height; the value given has been corrected for non-linearity of anemometer response. The number in brackets following the value of V_a/U is that of the anemometer used. Anemometers numbers 1 2 and 3 were in the inlet guide and numbers 4, 5 and 6 in the stator row (Figure 2).

TABLE VI

Calculated and experimental values of alternating stress

1. Rotor blades

Speed rev/min	V_a/U	No. of cells	Calc. stress[1] components *			Total calc.[2] stress *	Range of[3] observed stress *
4000	0.465	1	0.8(4)	0.5(5)		±1.3	±(1.15 - 1.25)
"	0.465	2	0.45(2)	1.25(2½)		±1.7	±(2.25 - 2.5)
"	0.295	1	0.66(4)	0.43(5)		±1.34	±(1.2 - 1.7)
4500	0.45	2	0.4(1)	0.75(2)	0.4(2½)	±1.55	±(1.7 - 1.9)
"	0.285	1	1.4(4)	0.36(5)		±1.76	±(1.5 - 2.5)
5000	0.44	2	0.85(1)	2.33(2)		±3.18	±(2.6 - 3.6)
"	0.305	2	0.83(1)	3.72(2)		±4.3	±(4.4 - 5.0)
5500	0.43	2	0.72(1)	2.01(2)		±2.73	±(1.8 - 2.4)
"	0.29	2	0.85(1)	2.15(2)		±3.0	±(1.4 - 2.5)

2. Stator blades

Speed rev/min	V_a/U	No. of cells	Calc. stress[1] components *		Total calc.[2] stress *	Range of[3] observed stress *
4000	0.465	1	0.5(5)		±0.5	±(0.9 - 1.3)
"	0.465	2	0.24(2)	0.22(2½)	±0.46	±(0.9 - 1.3)
"	0.295	1	0.3(1)	0.38(5)	±0.68	±(1.4 - 2.9)
4500	0.45	2	1.12(2)		±1.12	±(1.4 - 1.9)
"	0.285	1	1.1(5)		±1.1	±(1.0 - 2.2)
5000	0.44	2	0.32(1)	0.57(2)	±0.89	±(0.6 - 0.9)
"	0.305	2	2.75(2)		±2.75	±(1.8 - 2.5)
5500	0.43	2	0.37(1)	0.73(2)	±1.1	±(0.9 - 1.4)
"	0.29	2	0.50(1)	1.12(2)	±1.62	±(1.25 - 2.1)

Note:

* All stresses are given in tons/sq.in.

(1) Number in brackets following stress figure is that of the harmonic concerned.

(2) The figure given in this column is the arithmetic sum of the separate components shown in previous column except for 5000 rev/min V_a/U = 0.305, the figure given for this condition is phase corrected.

(3) The observed stress range is that of the alternating stress maxima encountered in a time interval of 1 second.

APPENDIX I

Information on the extracts from the records (Figures 11 to 18)

To illustrate this Report, extracts from the records obtained during this series of tests and from the multi-stage tests have been used. The information required to identify and understand these records is given below.

General

Identification of the trace on a particular record is by letter starting from the uppermost trace which is trace a.

Revolution and time marking

Channel f was used throughout for this purpose. In the single-stage recordings the downward deflections of this trace were caused by impulses derived from a crystal controlled oscillator at 500 c/sec, the upward deflections were from a revolution marking device giving a pulse every 1.186 revolutions. The revolution marking in the multi-stage recordings was taken from a standard tachometer completing 1 cycle every four revolutions of the main shaft.

Velocity perturbations

The number of the hot wire anemometer corresponding to a particular trace is given, from which its angular and axial position can be found by reference to Figure 2. The radial position is indicated as a fraction of rotor blade height. The average value of the maximum deviation from the mean velocity can be read in Table IV. The positions of the anemometers in the multi-stage compressor are given in Reference 5.

Alternating stress

The strain gauges on the stationary blades are numbered in accordance with Figure 2. Strain gauges on the rotor blades are lettered A, B, C and D.

FIGURE 11

		Channel	Source
1.	Record A3/17		
	4000 rev/min $V_a/U = 0.504$	a	S.G. 3
		b	S.G. 2
		c	Anemometer 4 (0.8)
		d	" 5 (0.25)
		e	" 6 (0.8)

FIGURE 11 (cont'd)

		Channel	Source
2.	Record A4/19		
	4000 rev/min V_a/U = 0.463	a	S.G.C.
		b	S.G.B.
		c	Anemometer 1 (0.8)
		d	" 2 (0.5)
		e	" 3 (0.8)
3.	Record A4/22		
	4000 rev/min V_a/U = 0.463	a	S.G.C.
		b	S.G.B.
		c	Anemometer 4 (0.8)
		d	" 5 (0.5)
		e	" 6 (0.8)

FIGURE 12

1.	Record B3/52		
	4500 rev/min V_a/U = 0.493	a	S.G.A.
		b	S.G.B.
		c	Anemometer 1 (0.8)
		d	" 2 (0.5)
		e	" 3 (0.8)
2.	Record B4/60		
	4500 rev/min V_a/U = 0.447	a	S.G.8.
		b	S.G.7
		c	Anemometer 1 (0.8)
		d	" 2 (0.5)
		e	" 3 (0.8)
3.	Record B4/63		
	4500 rev/min V_a/U = 0.447	a	S.G.3
		b	S.G.2
		c	Anemometer 4 (0.8)
		d	" 5 (0.5)
		e	" 6 (0.8)

FIGURE 13

1.	Record B4/62		
	4500 rev/min V_a/U = 0.447	a	S.G.A.
		b	S.G.B.
		c	Anemometer 4 (0.8)
		d	" 5 (0.5)
		e	" 6 (0.8)

FIGURE 13 (cont'd)

		Channel	Source
2.	Record B5/68		
	4500 rev/min V_a/U = 0.283	a b c d e	S.G.A. S.G.2 S.G.8 Anemometer 1 (0.8) " 4 (0.8)
3.	Record B6/74		
	4500 rev/min V_a/U = 0.179	a b c d e	S.G.A. S.G.2 S.G.8 Anemometer 3 (0.8) " 6 (0.8)

FIGURE 14

1.	Record C4/99		
	5000 rev/min V_a/U = 0.44	a b c d e	S.G.C. S.G.D. Anemometer 1 (0.8) " 2 (0.5) " 3 (0.8)
2.	Record C5/105		
	5000 rev/min V_a/U = 0.302	a b c d e	S.G.C. S.G.D. Anemometer 1 (0.8) " 2 (0.5) " 3 (0.8)
3.	Record C5/104		
	5000 rev/min V_a/U = 0.302	a b c d e	S.G.A. S.G.2 S.G.8 Anemometer 1 (0.8) " 3 (0.8)

FIGURE 15

1.	Record D4/145		
	5500 rev/min V_a/U = 0.432	a b c d e	S.G.C. S.G.4 S.G.8 Anemometer 1 (0.8) " 4 (0.8)

FIGURE 15 (cont'd)

	Channel	Source
2. Record D5/154		
5500 rev/min V_a/U = 0.293	a	S.G.C.
	b	S.G.4
	c	S.G.8
	d	Anemometer 1 (0.8)
	e	" 4 (0.8)
3. Record D6/161		
5500 rev/min V_a/U = 0.184	a	S.G.C.
	b	S.G.4
	c	S.G.8
	d	Anemometer 1 (0.8)
	e	" 4 (0.8)

FIGURE 16

1. Record D5/150		
5500 rev/min V_a/U = 0.293	a	S.G.C.
	b	Anemometer 1 (0.8)
	c	" 3 (0.8)
	d	" 4 (0.8)
	e	" 6 (0.8)

FIGURE 17

1. Record 9 from multi-stage tests		
4000 rev/min V_a/U = 0.285	a rotors	S.G.1
	b	S.G.2
	c 1st stage	Anemometer 1 (0.8)
	d stators	" 3 (0.8)
	e	" 6 (0.8)
2. Record A5/28		
4000 rev/min V_a/U = 0.292	a	S.G.A.
	b	S.G.B.
	c	Anemometer 4 (0.8)
	d	" 5 (0.5)
	e	" 6 (0.8)

FIGURE 18

		Channel		Source
1.	Record 37 from multi-stage tests			
	5700 rev/min V_a/U = 0.31	a		S.G.1
		b	rotors	S.G.2
		c	1st stage	Anemometer 1 (0.8)
		d	stators	" 3 (0.8)
		e		-
2.	Record D5/158			
	5500 rev/min V_a/U = 0.295	a		S.G.C.
		b		S.G.D.
		c		Anemometer 4 (0.8)
		d		" 5 (0.5)
		e		" 6 (0.8)

APPENDIX II

Theory of the hot wire anemometer

1.0 Steady flow

It was shown by King[9] that the rate of heat loss/wire length for a heated wire of diameter D could be expressed as follows:-

$$\frac{H}{T - T_E} = Ak + B\sqrt{\frac{K_p\,\mu}{k}\left(\frac{k^2\,\rho}{\mu}\right)\sqrt{V.D}} \qquad \ldots\ldots\ldots\ldots(1)$$

$$= F(pv) \qquad \ldots\ldots\ldots\ldots\ldots\ldots\ldots\ldots(2)$$

where A = constant

B = constant

K_p = specific heat at constant pressure

D = wire diameter

H = rate of heat loss/wire length

F(pv) = function of pressure and velocity

k = coefficient of heat conductivity

ρ = fluid density

V = velocity

p = pressure

μ = coefficient of viscosity

T = equilibrium temperature attained by heated wire in fluid stream

T_E = equilibrium temperature attained by unheated wire in fluid stream

Equating heat loss in a wire of length L with the heat produced by electrically heating the wire of resistance R with a current of 'I' amps we may write:-

$$I^2R = \left(T - T_E\right) L\, F(pv) \qquad \ldots\ldots\ldots\ldots\ldots\ldots(3)$$

If R_o is the resistance of the wire at a temperature T_o and if α_o is the temperature coefficient of resistance we may replace the temperatures T and T_E in Equation (3) with equilibrium resistance values for:-

$$R - R_E = R_o \alpha_o \left(T - T_E \right) \qquad \text{.....(4)}$$

Thus

$$I^2R = \frac{R - R_E}{\alpha_o R_o} \cdot L \cdot F(pv) \qquad \text{.....(5)}$$

$$F(pv) = \frac{I^2 R_o \alpha_o}{L} \left\{ \frac{R/R_E}{R/R_E - 1} \right\} \qquad \text{.....(6)}$$

Thus if for a given wire the resistance ratio is kept constant $F(pv)$ is proportional to the current square.

2.0 Rapid small flow fluctuations

If the hot wire is placed in an air stream in which small rapid flow fluctuations occur, then r_f is the perturbed nature of resistance corresponding to a velocity fluctuation.

Then

$$I^2 r_f = \frac{L}{\alpha_o R_o} \left(\bar{R} - R_E \right) I' \cdot r_f + \frac{L \bar{F} . r_f}{R_o \alpha_o} + \frac{cSL}{\alpha_o R_o} \cdot \frac{dr_f}{dt} \qquad \text{.....(7)}$$

where r_f = fluctuation in wire resistance

$$I' = \left[\frac{dF}{dv} \right]_p = \text{constant}$$

$\bar{F}$ = mean value of $F(pv)$

v = fluctuation of velocity

S = cross section area

c = specific heat/unit volume

Fluctuation in voltage across hot wire is given by Ohms Law.

$$e = IR$$

Thus

$$v = \frac{(L\bar{I} - I^2 R_0 a_0)\, e + cSL\, de/dt}{I L (R - R_e) F'} \qquad \ldots\ldots\ldots\ldots\ldots\ldots(8)$$

I being assumed constant

Thus for small fluctuations the velocity change is proportional to a certain linear combination of the hot wire voltage and the time derivative of the hot wire voltage. By incorporating a suitable compensation circuit the output of the amplifier e_1 may be such that:-

$$e_1 = G_1 e + G_2 de/dt \qquad \ldots\ldots\ldots\ldots\ldots\ldots\ldots\ldots\ldots(9)$$

where e is the hot wire voltage and G_1 and G_2 are proportional to the equivalent terms in (8). In this case the amplifier output is directly proportional to the velocity change.

3.0 Large flow fluctuations

In the presence of large flow fluctuations, so large as to markedly change the effective instantaneous resistance ratio, the treatment given in Section 2.0 is no longer valid. Under these conditions it is difficult to calculate a pressure velocity change but if limits of accuracy are maintained as within 10 per cent of the mean velocity change then an approximate method becomes available.

We have from King's formula and Equation (6)

$$\left.\begin{aligned} A + B\sqrt{pV'} &= \frac{R'/R_E}{R'/R_E - 1} \cdot f(I') \\ A + B\,(pV'') &= \frac{R''/R_E}{R''/R_E - 1} \cdot f(I'') \end{aligned}\right\} \qquad \ldots\ldots\ldots\ldots\ldots\ldots(10)$$

where V' and V'', R' and R'', I' and I'' are the perturbed values of velocity, resistance and current.

$f(I)$ is a function of current and can include any end conduction factors which may have to be considered[10].

Since the maintenance of a constant current is a feature of the hot wire anemometer system used we may put $f(I') = f(I'')$.

Thus neglecting A for the required accuracy.

In (10) we have:-

$$\frac{V'}{V''} = \left\{ \frac{R'/R_E / \left(R'/R_E - 1\right)}{R''/R_E / \left(R''/R_E - 1\right)} \right\}^2 \quad \ldots\ldots\ldots\ldots(11)$$

or if $V' = \bar{V}a + \Delta V$ and $V'' = \bar{V}a$

(11) may be rewritten as:-

$$\frac{\Delta V}{Va} = I - \left\{ \frac{R'/R_E / \left(R'/R_E - 1\right)}{\bar{R}/R_E \left(\bar{R}/R_E - 1\right)} \right\}^2 \quad \ldots\ldots\ldots\ldots(12)$$

The end conduction terms which have to be considered in f(I) could be readily calculated but are of minor significance in the present case and are therefore omitted.

In a flow where large perturbations occur the instantaneous resistance ratio is calculated and substituted in equation (12). Then large perturbations are readily evaluated.

APPENDIX III

Alternating blade stress and fluctuating airflow

1.0 Introduction

The response of the rotating blade to flow fluctuations along its length cannot strictly be calculated unless the phase, magnitude and harmonic content of the flow fluctuations are known along the blade length and the dynamic response of the blade is also known. These are in general not known so that some approximate method of computation must be adopted. Of necessity one has to divide the test results into three main types. In the first type the flow is such that the rotor stage is badly stalled and large flow fluctuations are present, in the second type the flow fluctuations are comparatively regular and arise through rotating stall cells, in the third type the rotor stage is operating at or near its design point and the flow fluctuations are ordered but small and spasmodic. The regions of flow are not clearly marked and there are bands of unstable flow conditions in between the three regions.

2.0 Alternating stress

The gas bending stress arises through the work done by the blades upon the air passing through the row. If the mean measured temperature rise through the rotor stage is ΔT then for a given blade the gas bending stress (q) is given by:-

$$q = M\Delta T \quad \text{where } M \text{ is a constant}$$

If we consider the conditions on mean diameter we have[11]:-

$$\frac{Kp\ \Delta T}{U^2} = \frac{Va}{U}\ (\tan \alpha_1 - \tan \alpha_2)$$

and

$$\frac{U}{Va} = \tan \alpha_0 + \tan \alpha_1$$

where

Kp = specific heat at constant pressure

ΔT = stage temperature rise

U = peripheral speed at mean diameter

Va = mean axial velocity

α_0 = air angle from inlet guide vanes

α_1 = inlet air angle to rotor

α_2 = outlet air angle from rotor

If we assume that the flow fluctuations may be regarded as fluctuations in the mean axial velocity then by differentiation we may write:-

$$\frac{\Delta q}{q} = \frac{\Delta V}{Va} \left\{ 1 - \frac{P\,U^2}{Kp\Delta T} \right\}$$

where $$P = \frac{d\,(\tan \alpha_1 - \tan \alpha_2)}{d\,(\tan \alpha_1)}$$

Both Δq and ΔV however are harmonic components.

Thus

$$\Delta q = \bar{\Delta} q \cos 2\pi f t$$

and $$\Delta V = \sum_{n=o}^{n=\infty} \bar{\Delta} V_n \cos nt$$

Thus to calculate the maximum alternating stress at the blade frequency the harmonic content of the exciting disturbances must also be known. The way of approach which provides the easiest method is that of alternating current theory where the response of a tuned damped circuit to an exciting frequency is well known[6].

If L is the inductance; R the resistance and C the capacity connected in series in an electric network then i' the quantity of charge flowing in the circuit is given by:-

$$L \frac{d^2 i'}{dt^2} + R \frac{di'}{dt} + \frac{i'}{C} = E_0 \cos nt$$

At resonance $n = \omega$ where ω is the natural frequency of the circuit and the voltage across the inductance and condensor is $\frac{1}{R}$ times the applied voltage. Where $n \neq \omega$ the response of the circuit can still be calculated from the universal response curve.

In mechanical systems the differential equation has a similar form but the two cases namely low and high rotational speeds must be considered separately for the rotating blade.

2.1 Low speed operation

At low rotational speeds the blade moves to some extent in its root fixing, we shall assume that this is affecting a rolling action when the blade vibrates so that if I is the moment of inertia of the blade, d the combined root damping and air damping and K the Coulomb damping we have:-

$$I\ddot{\theta} + d\dot{\theta} + K\theta = \sum_{n=o}^{n=\infty} F \sin nt$$

ρ = density

V = velocity

C = chord

C_F = aerodynamic force coefficient

α_1 = air inlet angle

ℓ = length of the blade

$$d_A = \text{air damping} = \frac{1}{2}\left[\rho V C \frac{\partial C_F}{\partial \alpha_1}\right]_m \frac{\ell^3}{3}$$

d_R = root damping

$d = d_A + d_R$

The sharpness of the response peaks "Q_L" may then be calculated as follows:-

$$Q_L = \frac{2\pi f \cdot I}{d} = \frac{mk^2 \cdot 2\pi f}{d_A + d_e}$$

where f = the natural frequency of the blade

mk^2 = the moment of inertia of the blade

Q_L = the response

2.2 High speed operation

At high speed the movement in the root fixing is negligible so we may consider the whole damping to arise from the air damping and the equation of motion becomes:-

$$M\ddot{x} + d_A\dot{x} + kx = \sum_{n=0}^{n=\infty} F \sin nt$$

where M is the effective mass of the blade.

The sharpness of the response peak 'Q_H' may then be calculated as follows:-

$$Q_H = \frac{M \cdot 2\pi f}{d_A}$$

The 'Q' factor can be considered as the stress magnification factor, the experimental value of ten found for Q with a blade of similar mass, root and aerodynamic form was used throughout the calculations at medium speeds.

2.3 Weighting factor

The distribution of the flow fluctuations over the blade length is not uniform but increases greatly from mean diameter to rotor tip when the rotor stage is partially stalled at speeds greater than one-third design speed. A weighting factor must then be introduced to convert the flow fluctuation measured at 0.8 blade length to an equivalent perturbation over the whole blade. A factor of 0.83 was chosen as a weighting factor at speeds greater than one-third design speeds. Below that speed no weighting factor was assumed.

3.0 Analysis of hot wire records

3.1 Random fluctuations - low speed

The treatment outlined in the previous paragraphs assumes that the frequency distribution of the disturbances is known. At low speeds (less than one-third design speeds) this is not true, for the fluctuations are random and irregular so that a complete harmonic analysis becomes impossible. Accordingly the fluctuations were meaned over intervals of approximately a half period of blade vibration for four engine revolutions, the root mean square deviation was then found. This method of sampling includes all frequencies from about zero to that of blade frequency so that the assignment of a response to this broad band is of doubtful validity. After consideration of this band width an effective value of 'Q' of 1.0 was assumed.

3.2 Random fluctuations - medium speed

At medium speeds the "random fluctuations", when the stall cell fluctuations break down, were analysed using a third octave filter tone spectrometer. The distribution of energy in the frequency bands near the blade frequency was then considered to yield an effective Q of three. This effective Q of three was then used in the analysis of the few points on the medium speed when the stall cell formation broke down into unsteady flow pulsation.

3.3 Rotating stall cell fluctuations

When rotating stall cells were present the harmonic content of the flow fluctuation was fairly accurately known so that the effective 'Q' for the first and second stall cell orders could readily be calculated as stated in paragraph 20. The Q, assumed at resonance, was taken as ten from another test upon a blade of similar weight, frequency, aerodynamic design and root fixing.

4.0 Aerodynamic considerations

Since the aerodynamic response of the rotor blade to flow fluctuation is unknown, the factor 'P' is unknown; we have therefore to assume suitable values. Where the first stage is badly stalled at and below 34 per cent design speed an arbitrary value of ten is assumed. Where the rotor blade only partially stalled we shall assume that the vector mean angle is effectively unchanged. With this latter condition P becomes equal to 2.

5.0 Conclusion

The whole approximate analysis can then be written -

$$\frac{\Delta q}{q} = \frac{\overline{\Delta V}}{\overline{V}_a} \cdot Q' \,(W.F) \quad \left(1 - P \frac{U^2}{Kp\ \Delta T} \right)$$

where Δq = alternating blade stress

q = steady gas bending stress

ΔV = fluctuation in mean axial velocity

Q' = effective stress magnification

$W.F$ = weighting factor

P = ratio between differential coefficients $\dfrac{d\,(\tan \alpha_1 - \tan \alpha_2)}{d\,(\tan \alpha_1)}$

U = mean diameter rotational speed

Kp = specific heat at constant pressure

ΔT = stage temperature rise

FIG. 1.

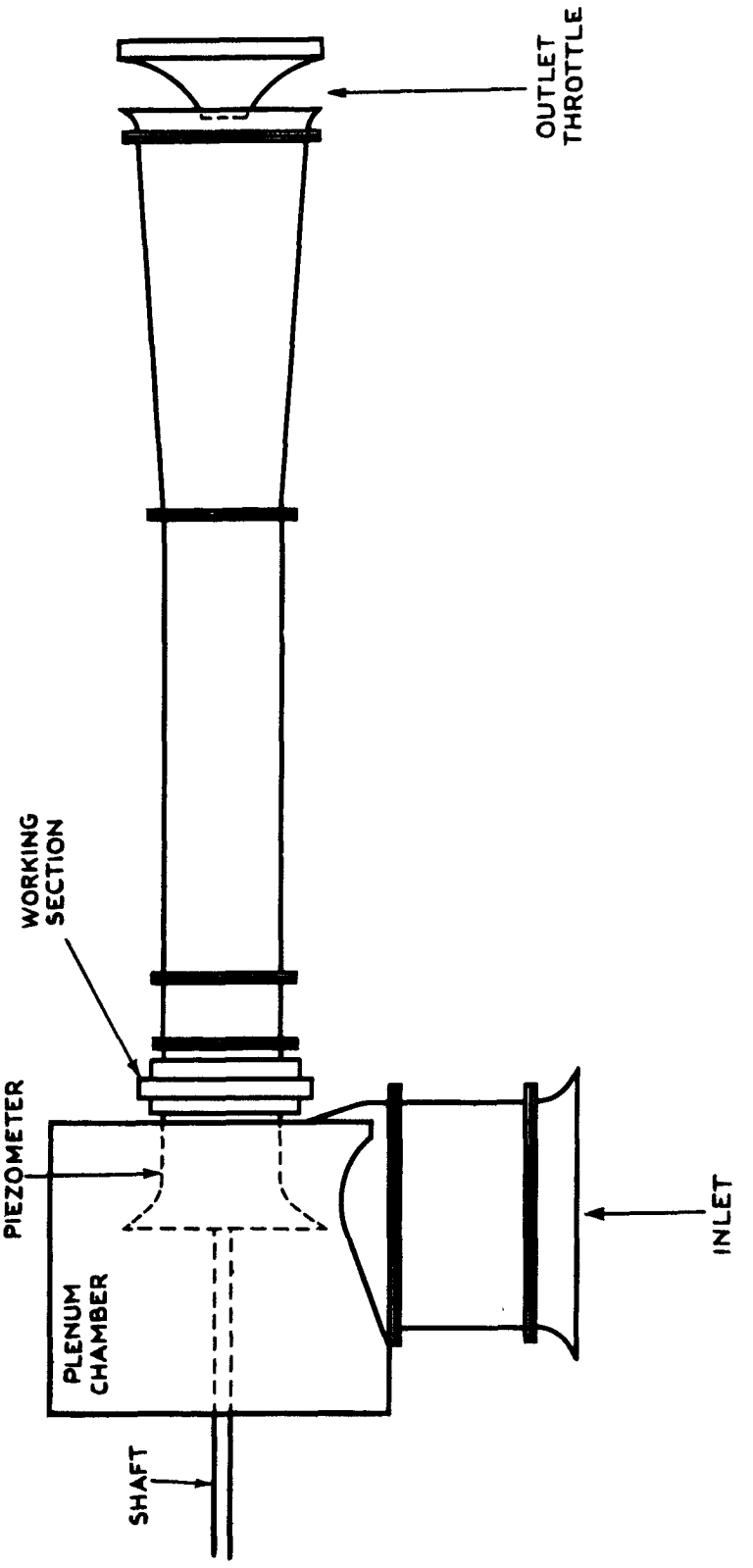

SINGLE STAGE RIG.
GENERAL ARRANGEMENT

FIG.2.

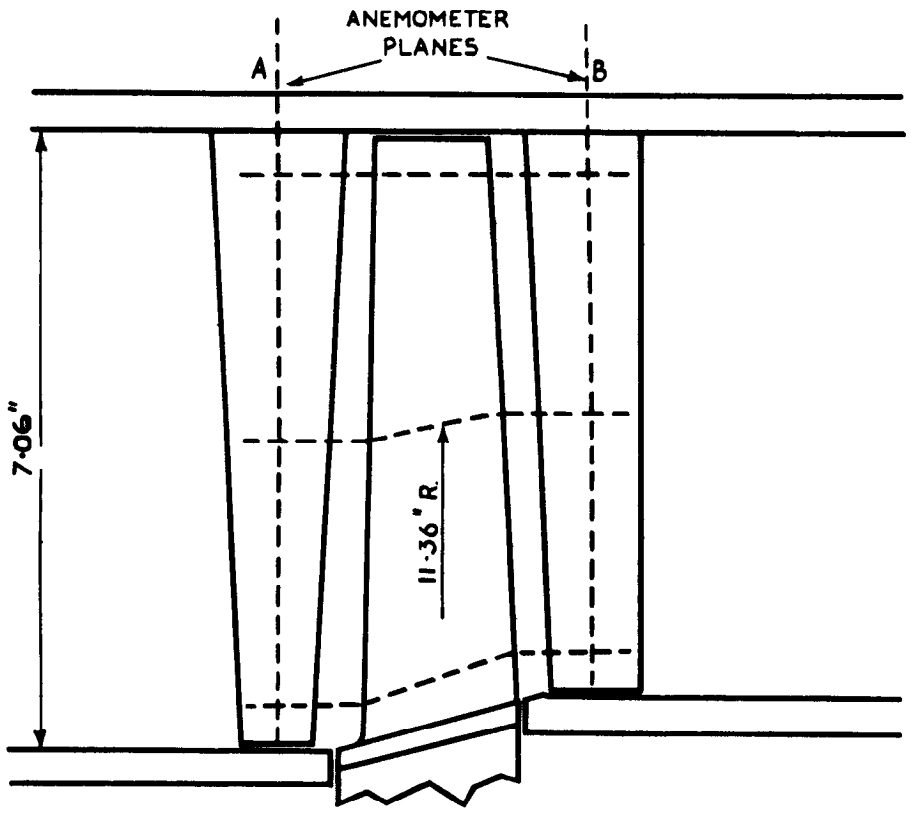

(A) WORKING SECTION.

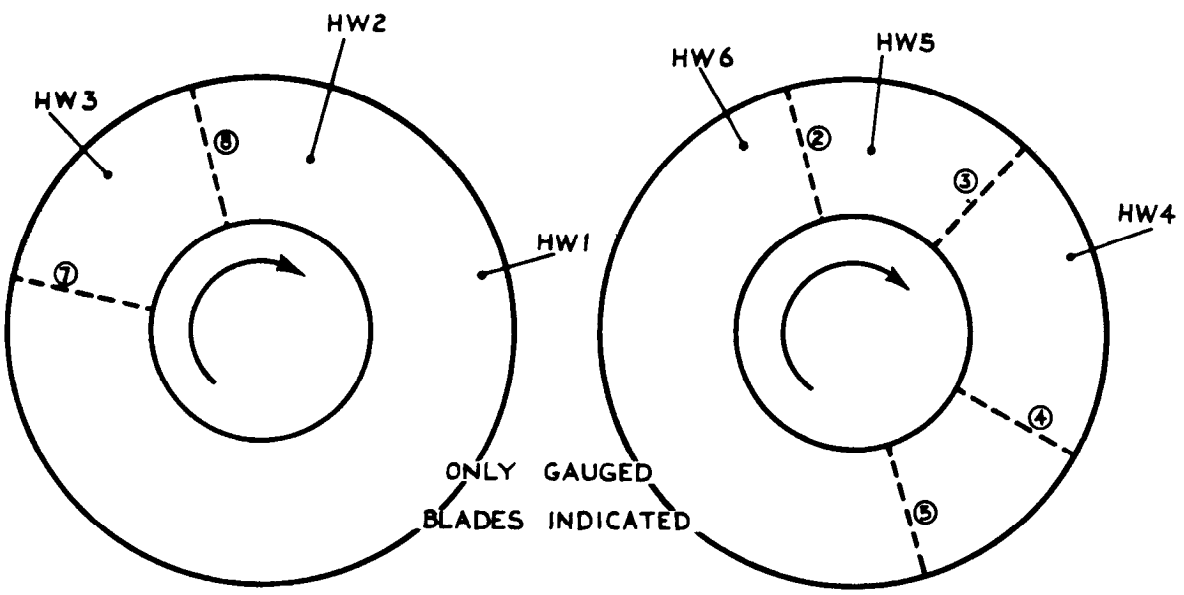

SECTION A SECTION B

(B) ANEMOMETER AND STRAIN GAUGE LOCATIONS.

FIG. 3

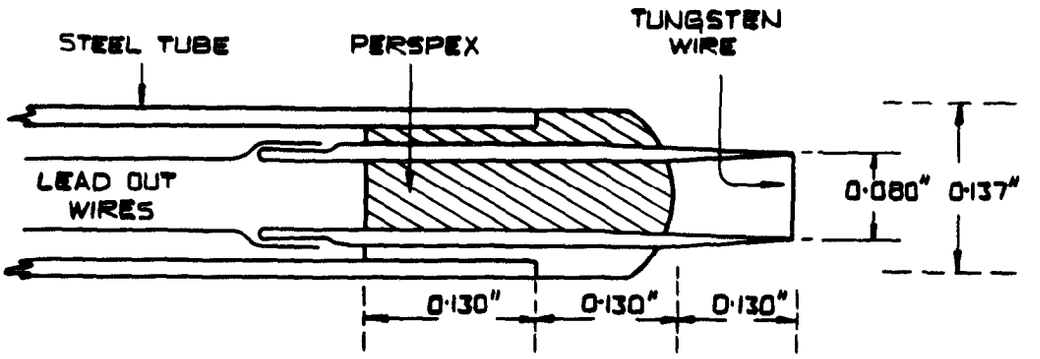

3A ANEMOMETER DETAILS.

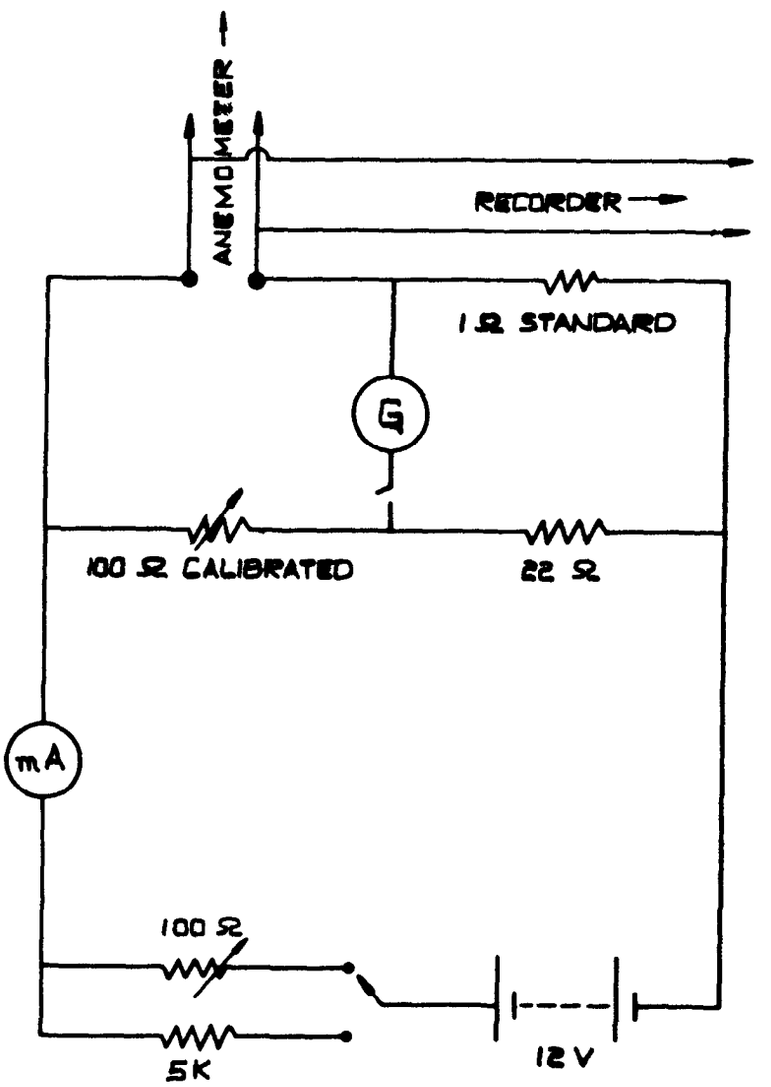

3B SUPPLY CIRCUIT.

FIG. 4.

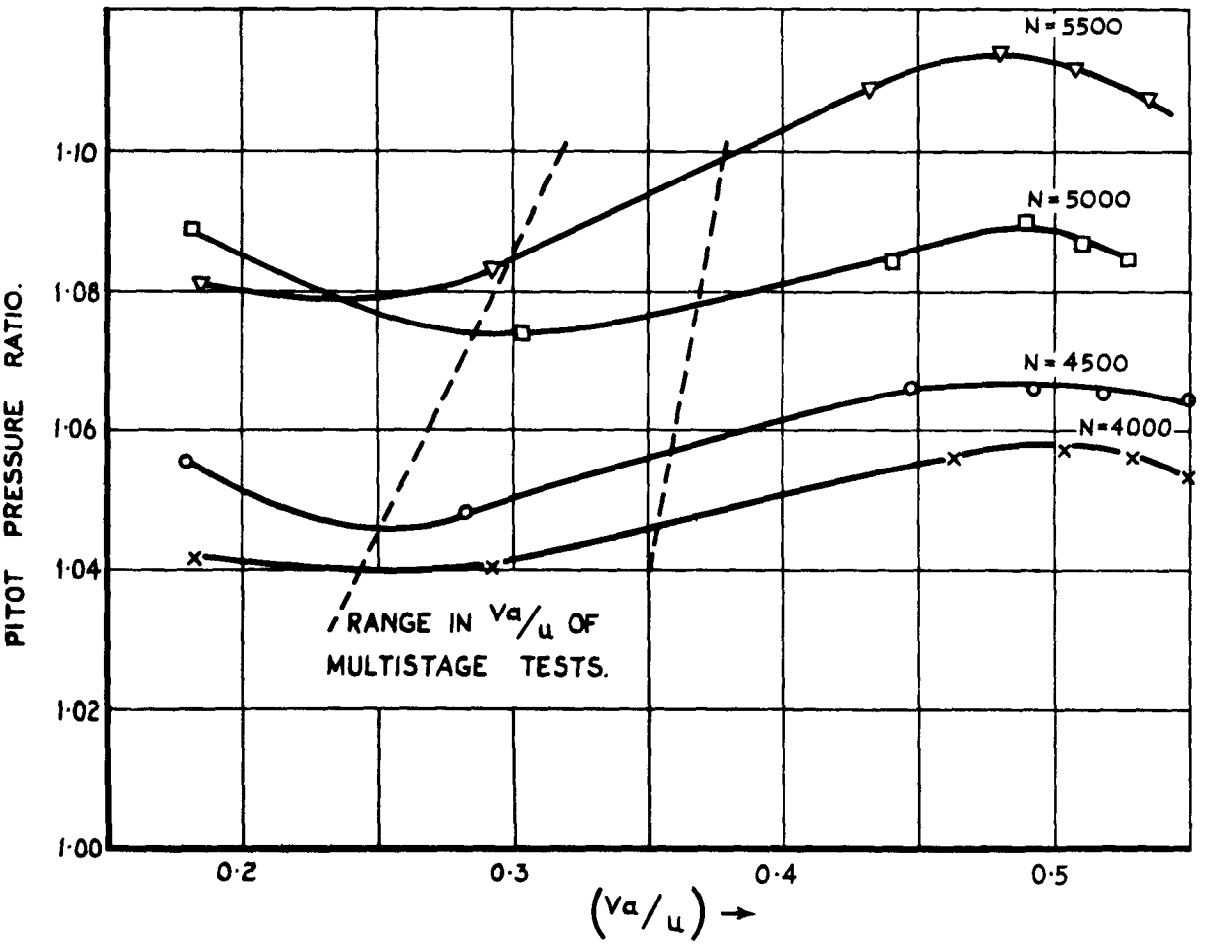

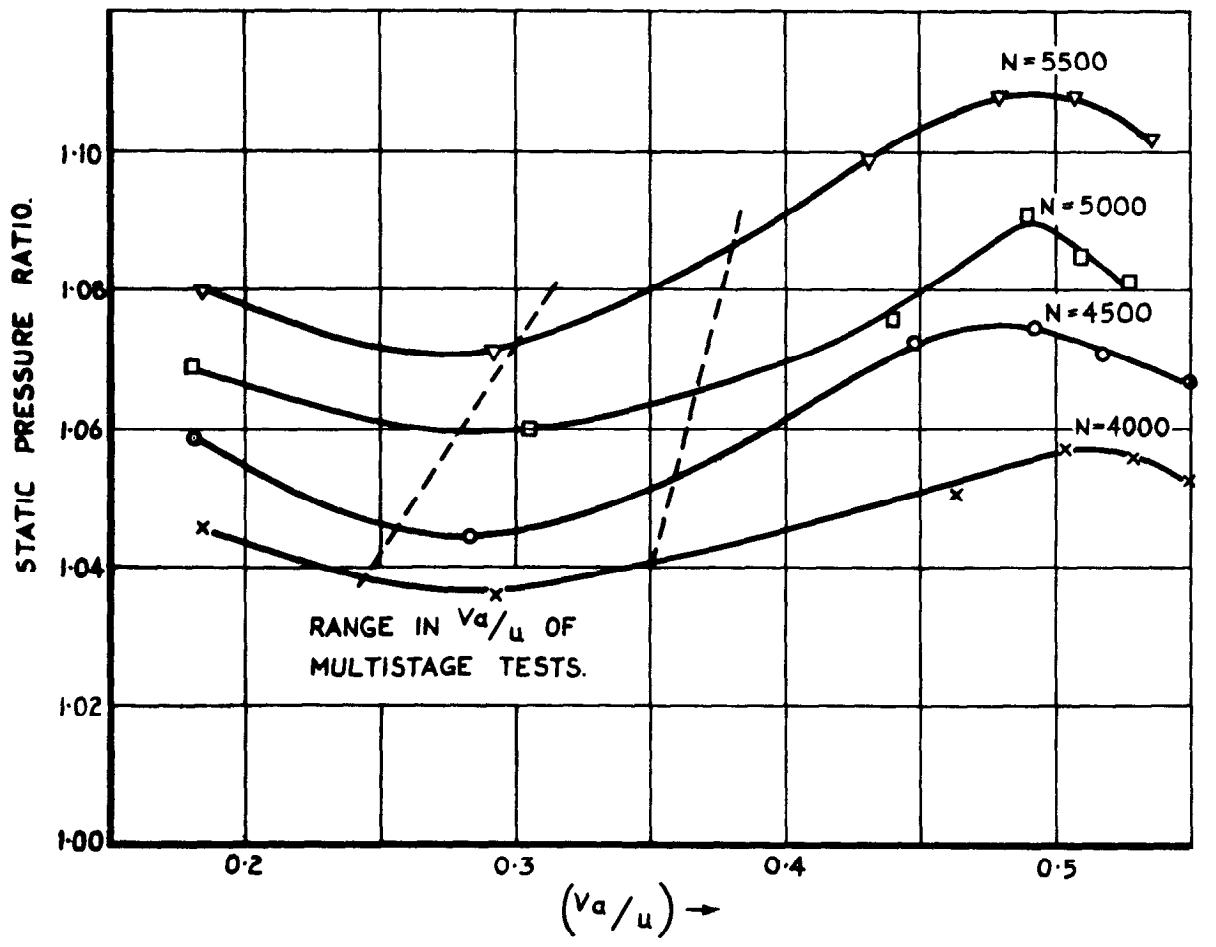

COMPRESSOR CHARACTERISTICS.

FIG. 5.

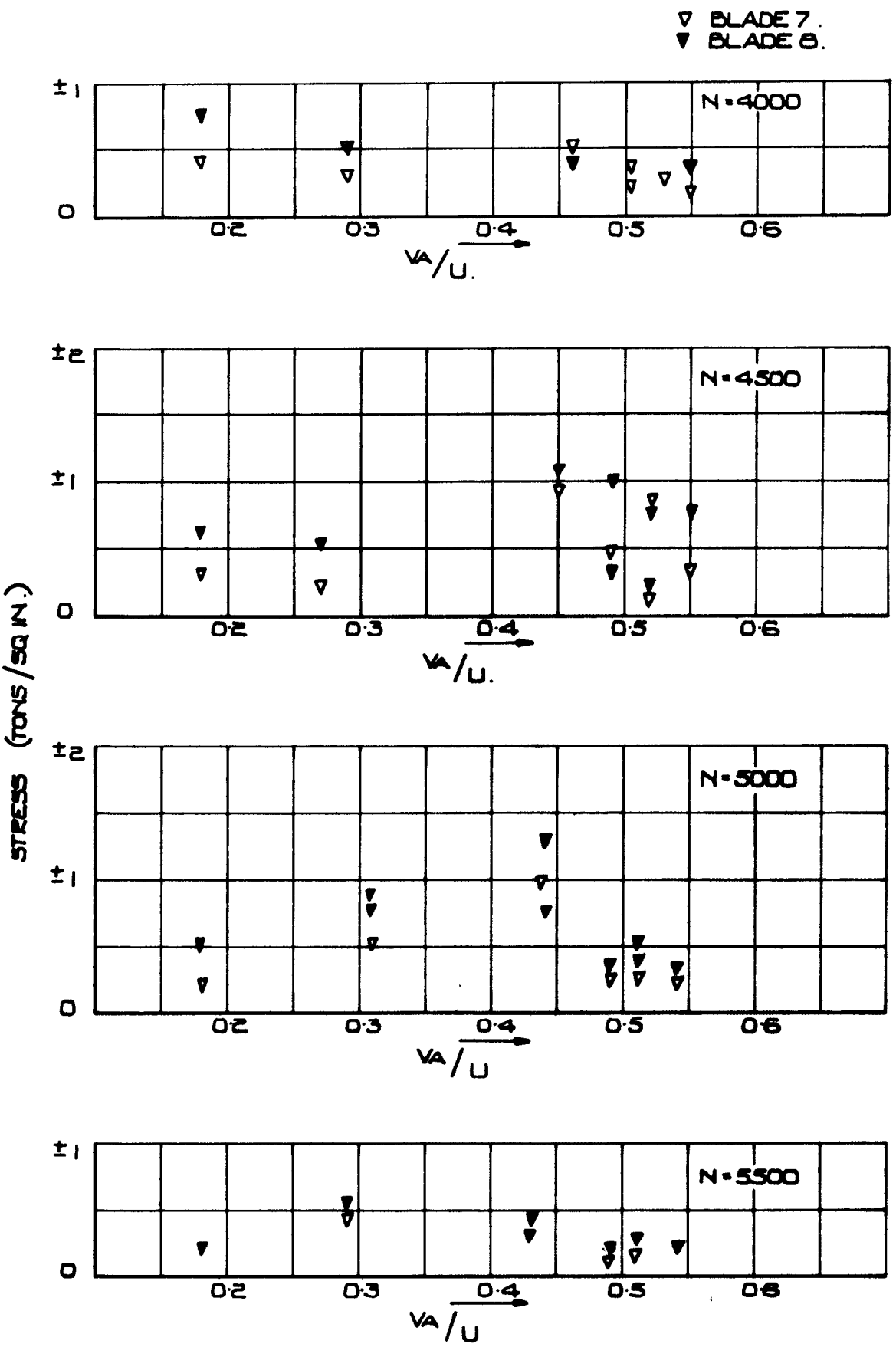

I.G.V. ALTERNATING STRESSES.

FIG. 6

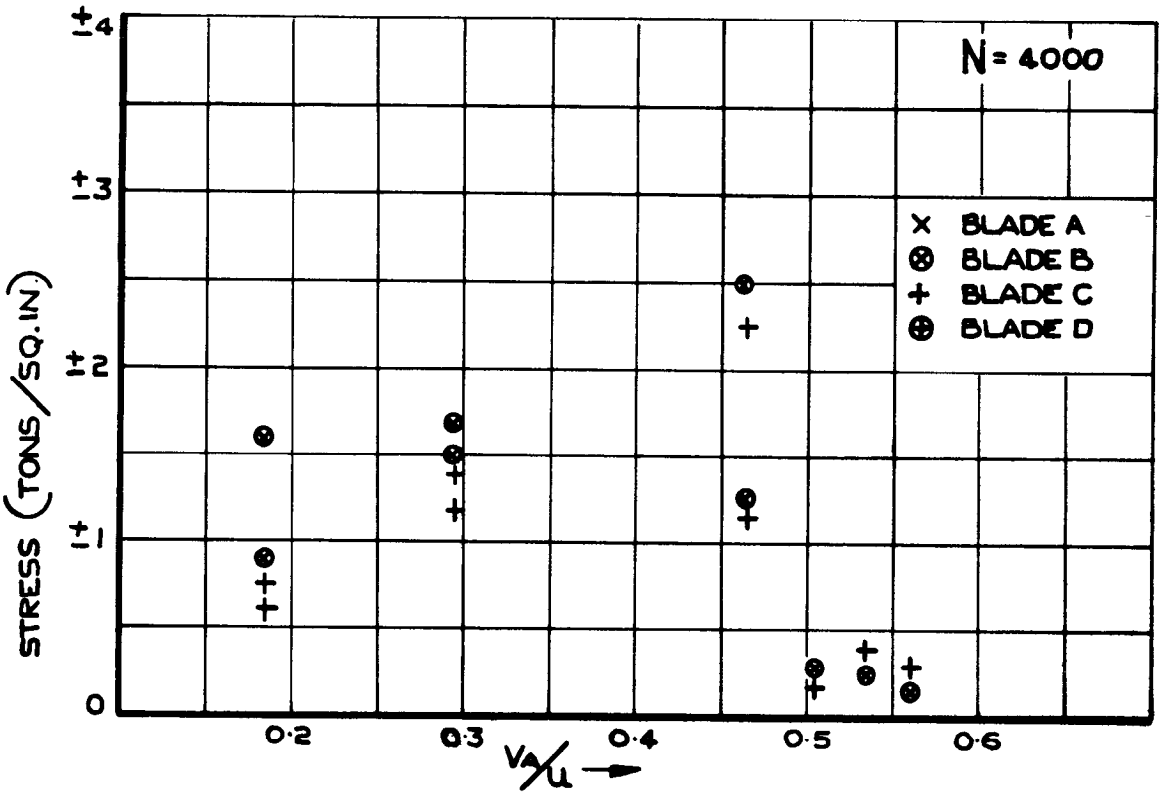

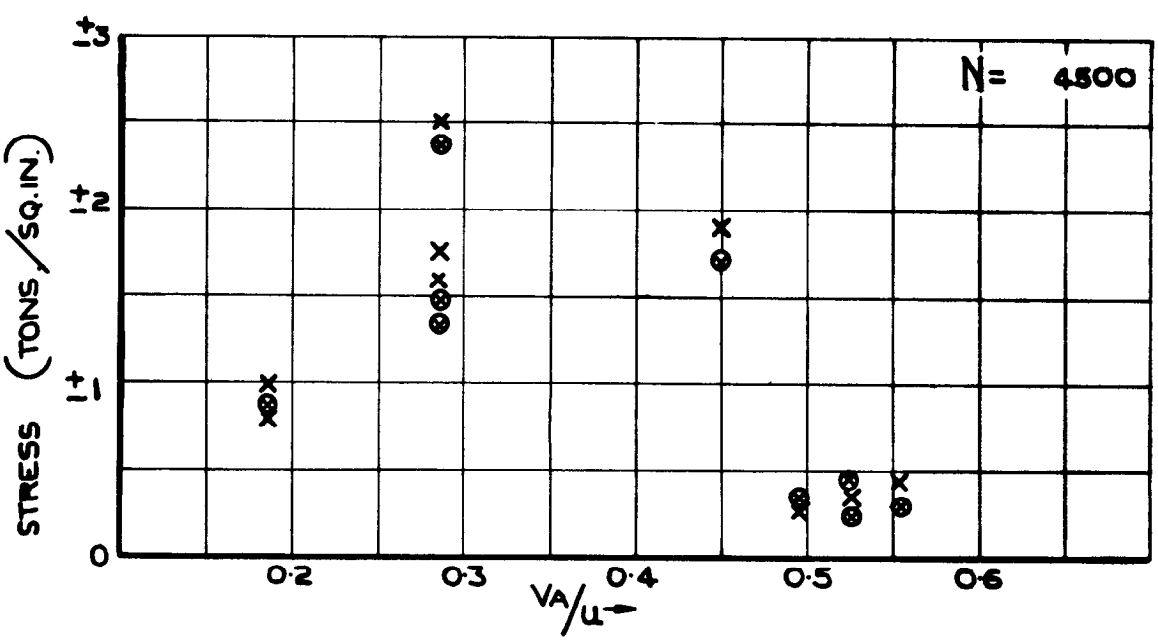

ROTOR BLADE–ALTERNATING STRESSES.

FIG.7

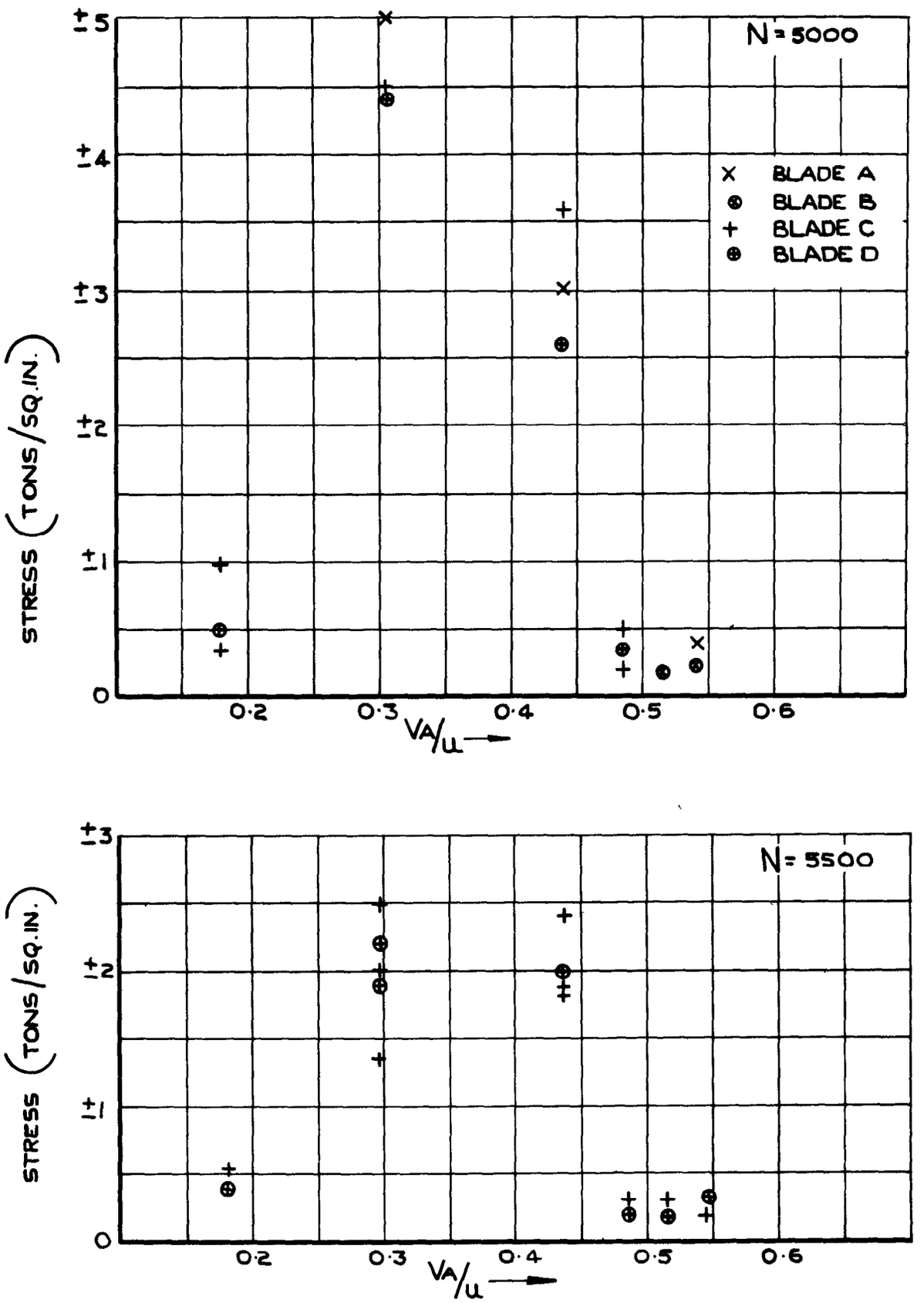

ROTOR BLADE – ALTERNATING STRESSES.

FIG. 8

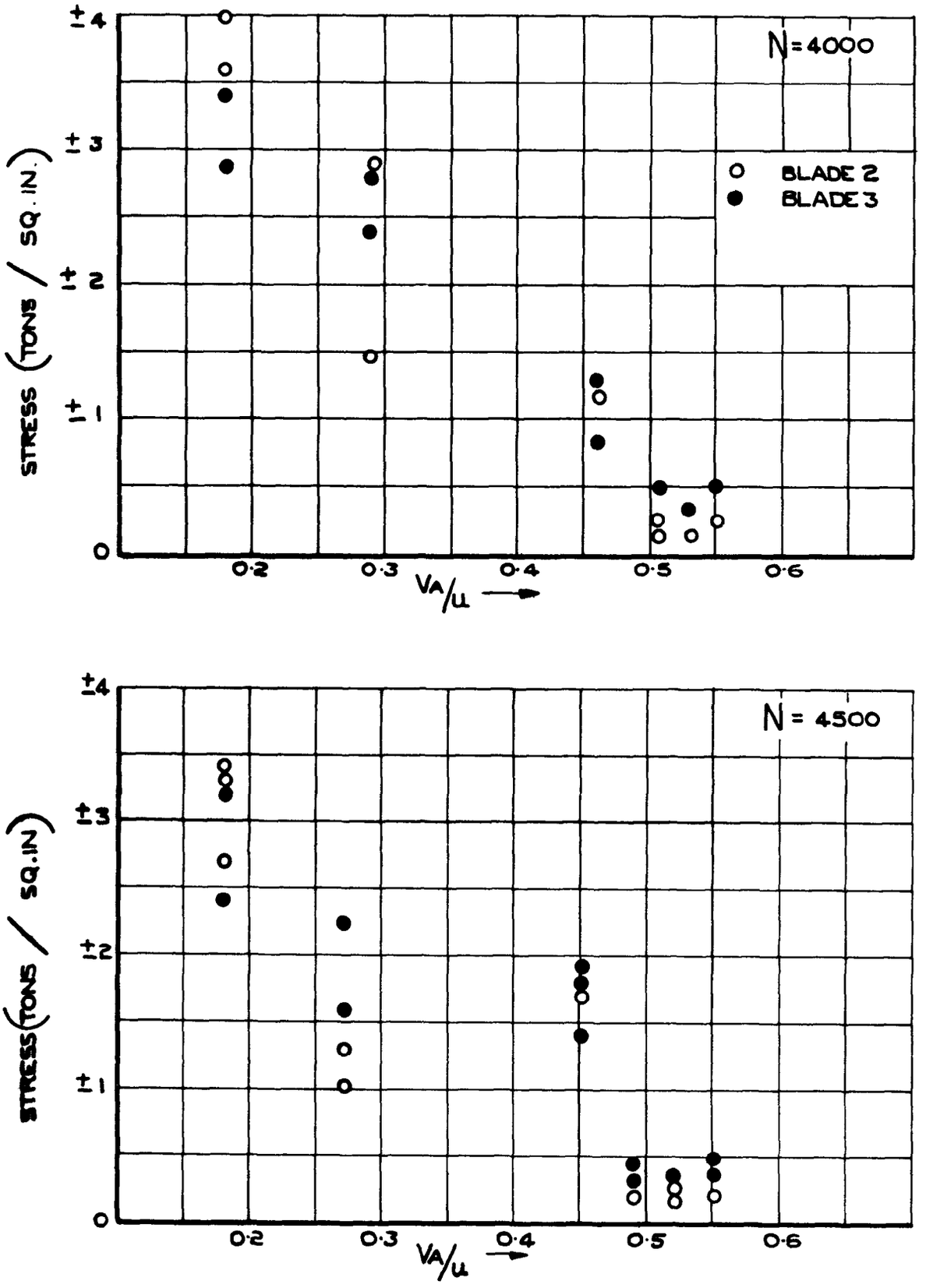

STATOR BLADE–ALTERNATING STRESSES.

FIG.9

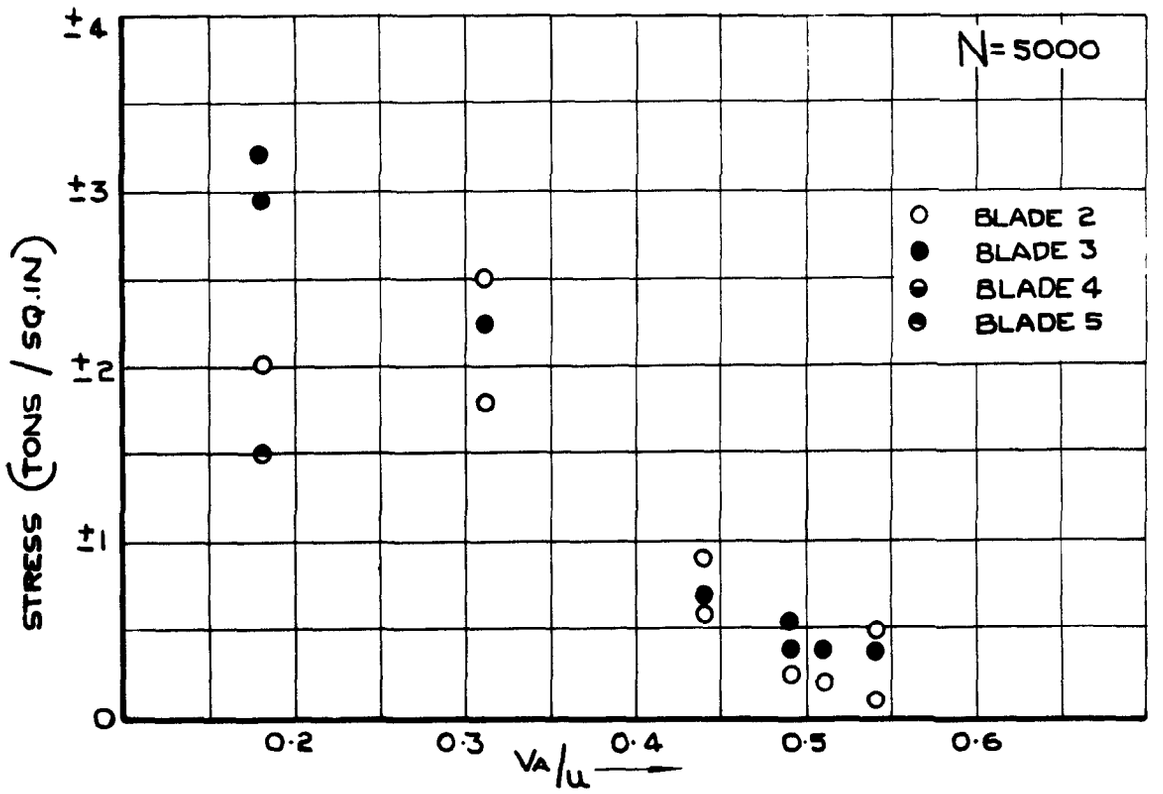

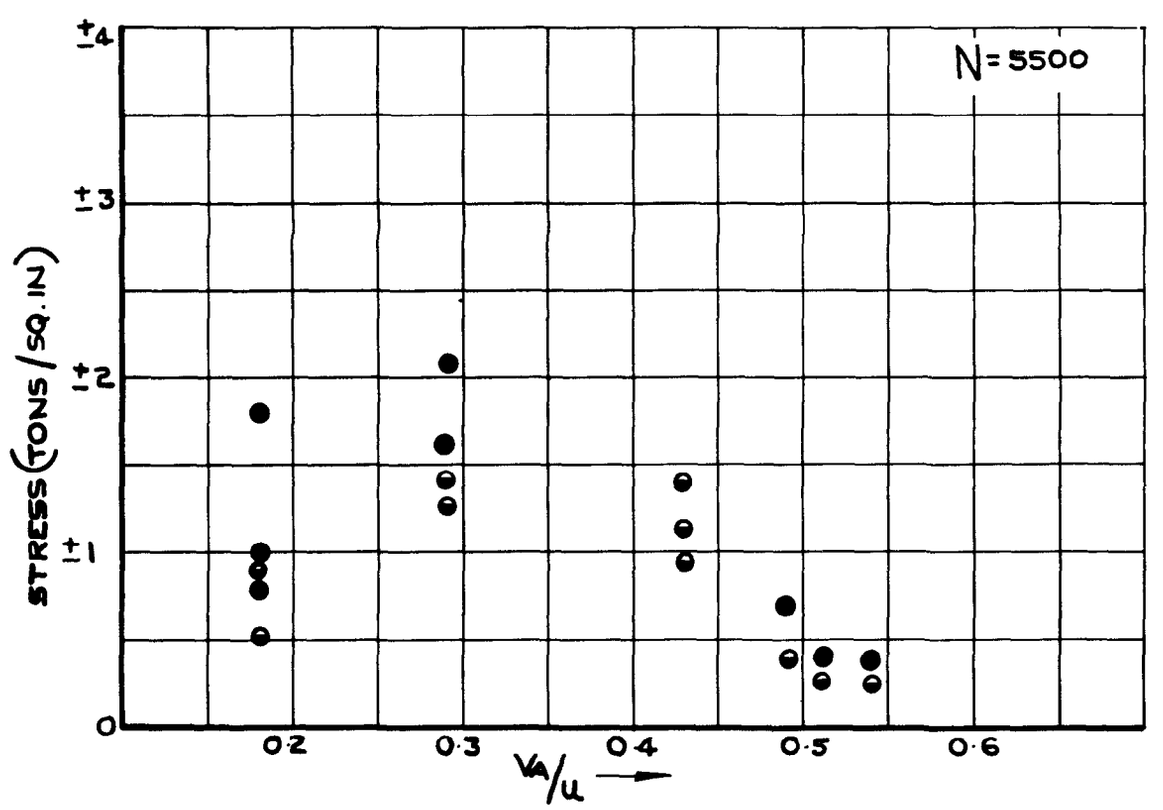

STATOR BLADE-ALTERNATING STRESSES.

FIG. 10

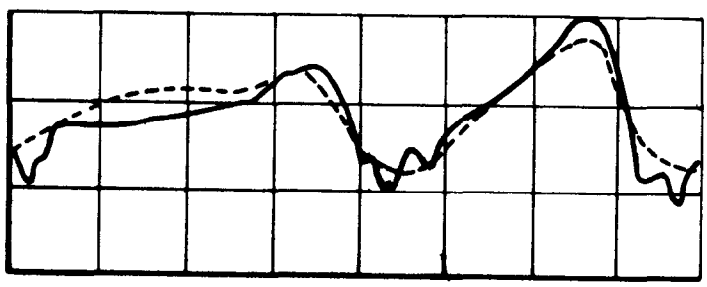

4000 REV/MIN V_a/ω = 0·463

4000 REV/MIN V_a/ω = 0·293

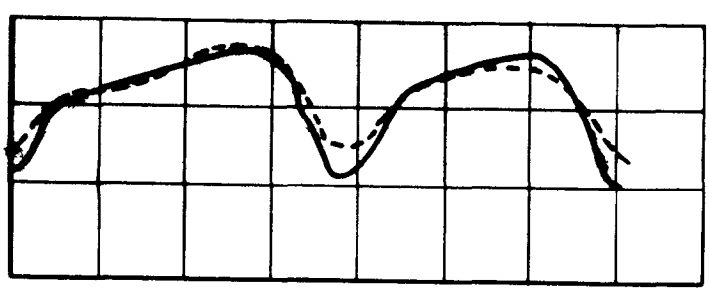

4500 REV/MIN V_a/ω = 0·447

——— TRACED ENLARGEMENT

– – – – – BUILT-UP WAVE FORM

HARMONIC ANALYSIS OF STALL CELL FORMS

FIG. 11

REP. 29

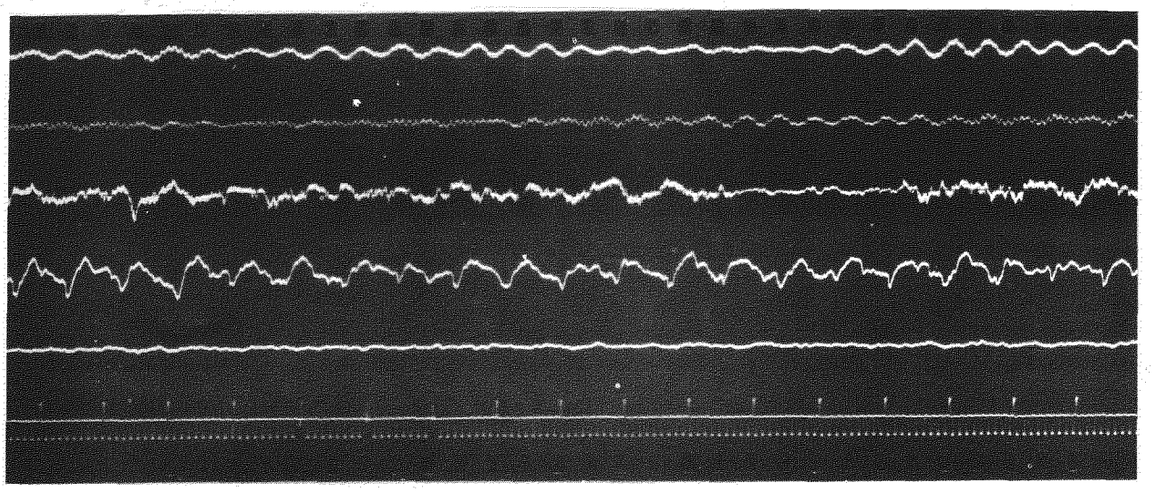

A3/17 $V_A/U = 0.51$

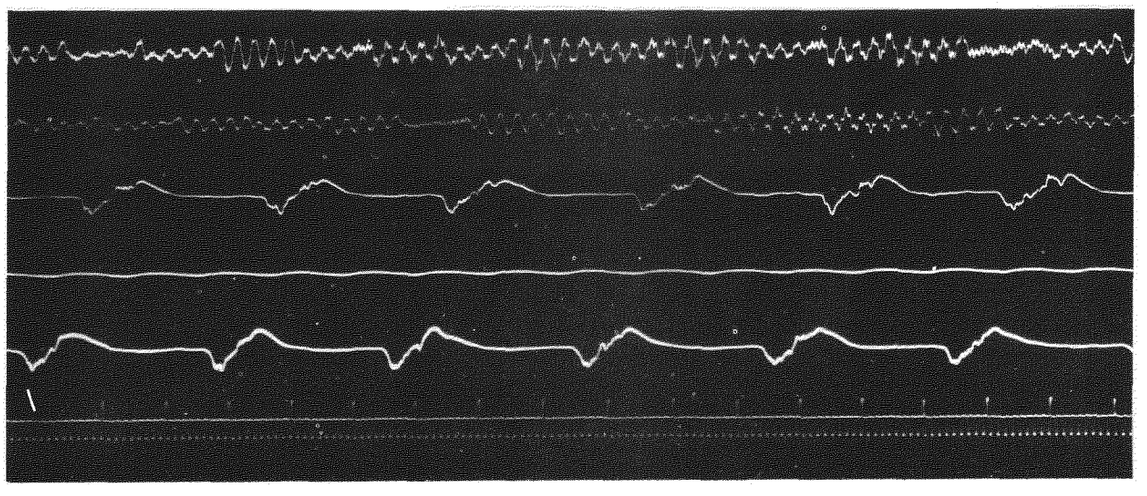

A4/19 $V_A/U = 0.465$

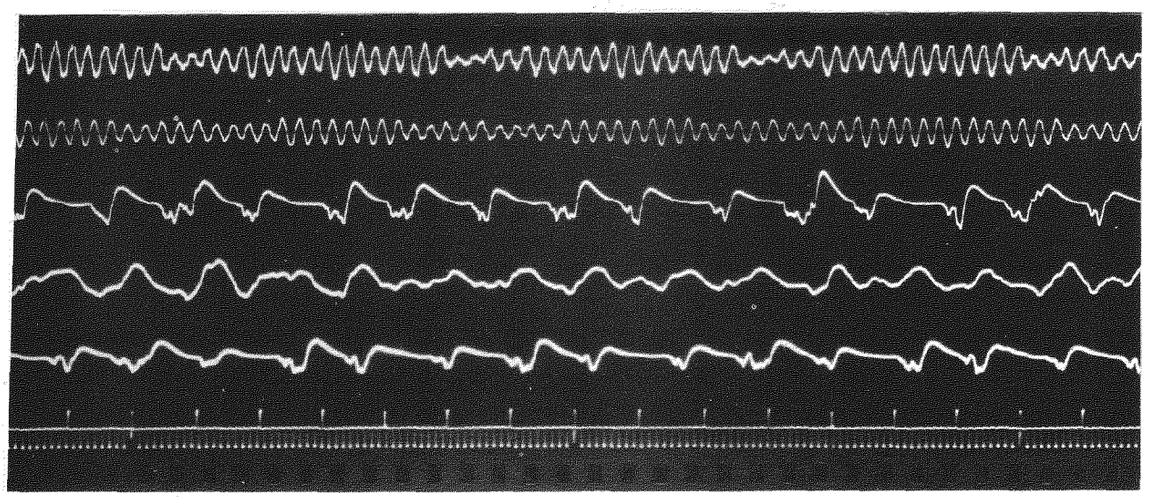

A4/22 $V_A/U = 0.465$

RECORDS AT 4000 R.P.M.

FIG. 12

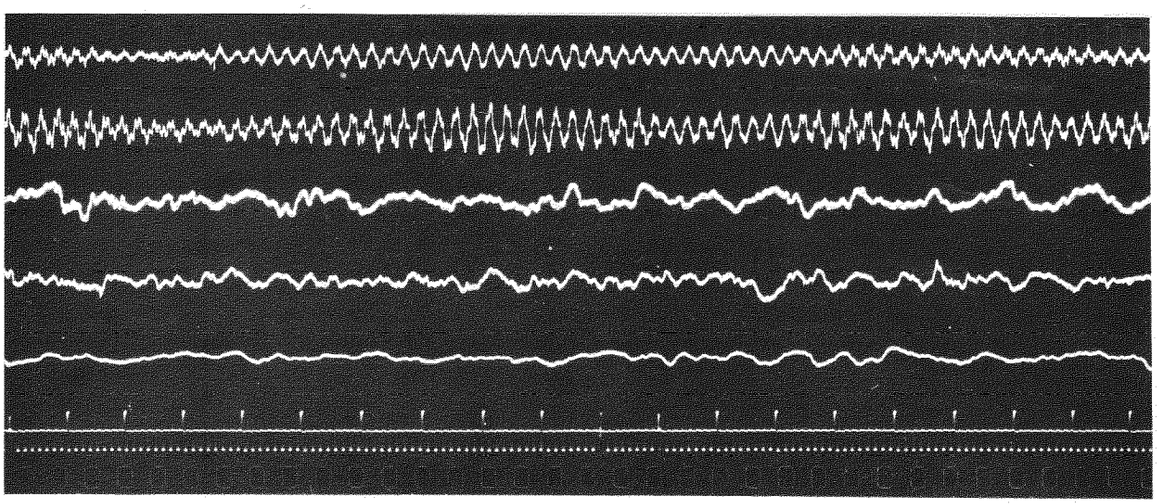

B3/52 $V_A/U = 0 \cdot 493$

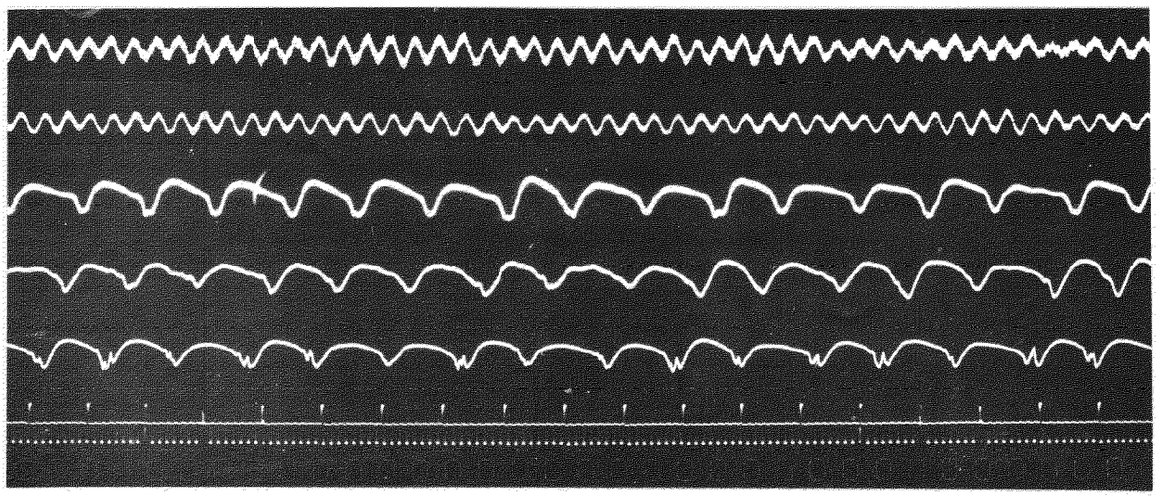

B4/60 $V_A/U = 0 \cdot 447$

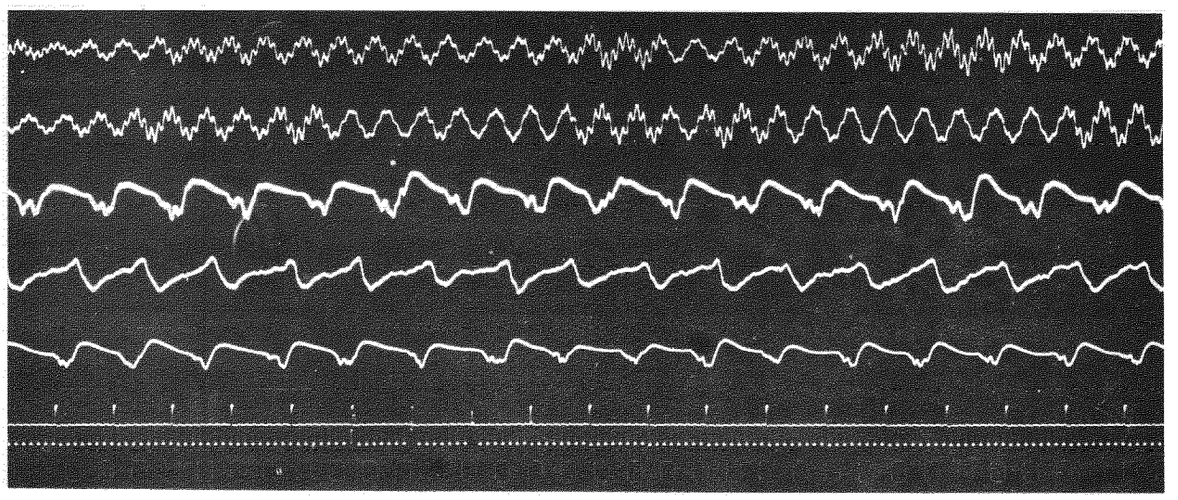

B4/63 $V_A/U = 0 \cdot 447$

RECORDS AT 4500 R.P.M.

FIG. 13

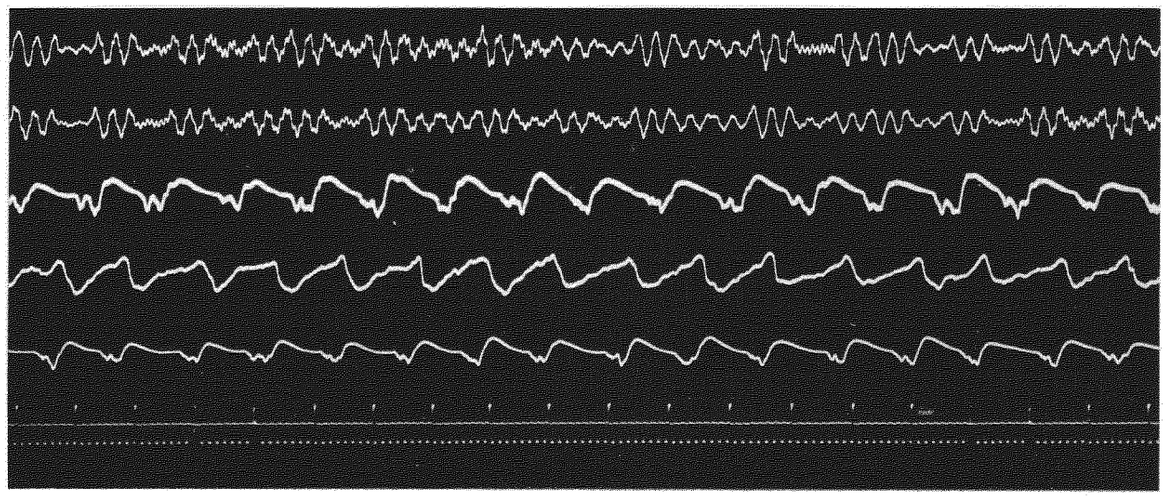

B4/62 $V_A/U = 0 \cdot 447$

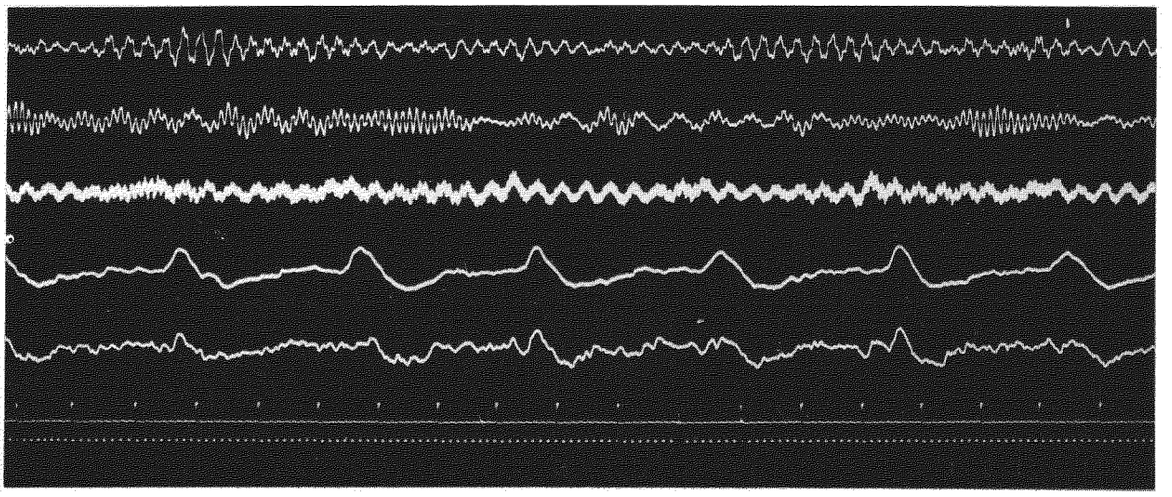

B5/68 $V_A/U = 0 \cdot 283$

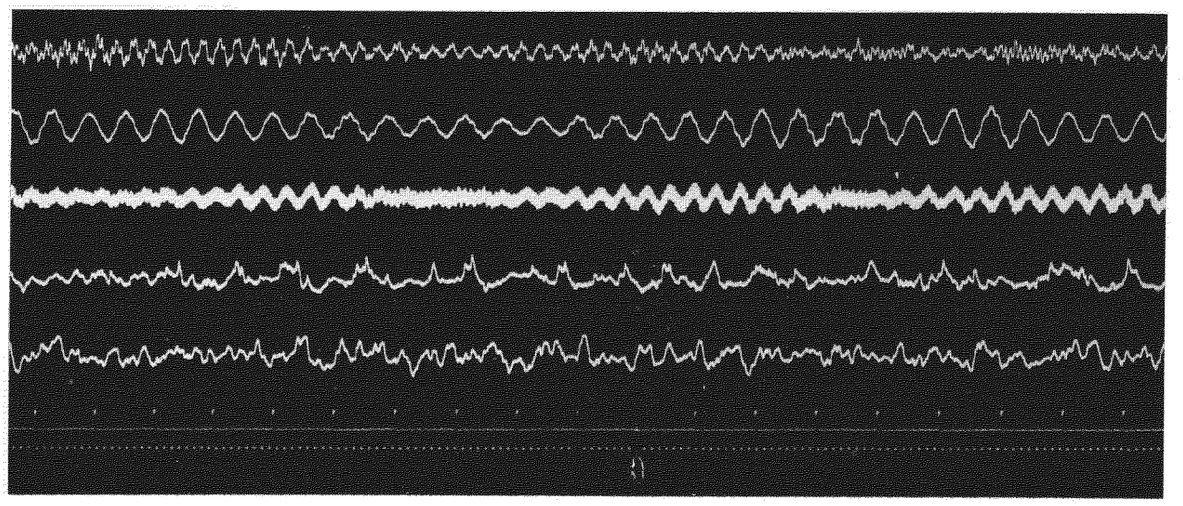

B6/74 $V_A/U = 0 \cdot 179$

RECORDS AT 4500 R.P.M.

FIG.14

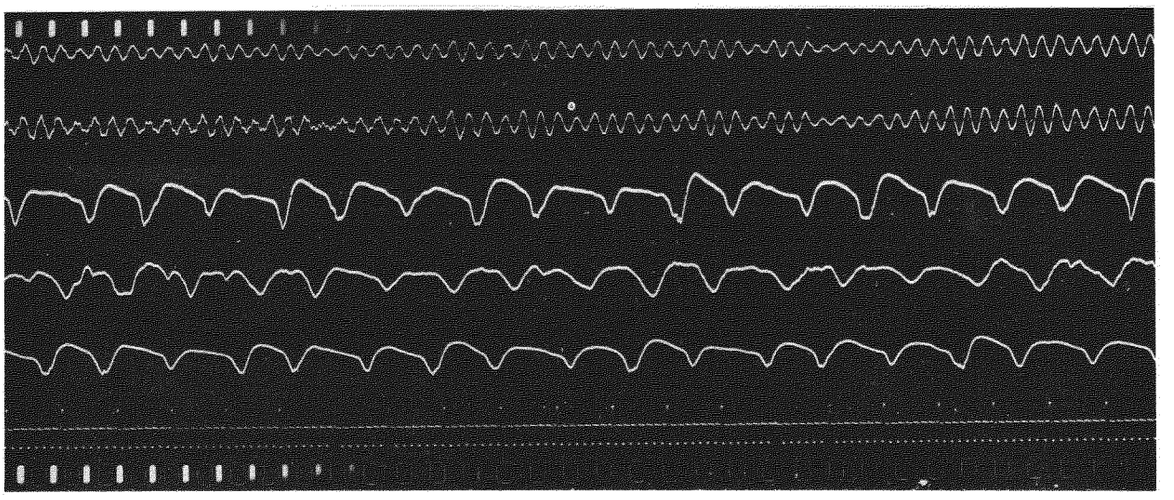

C4/99 $V_A/U = 0{\cdot}440$

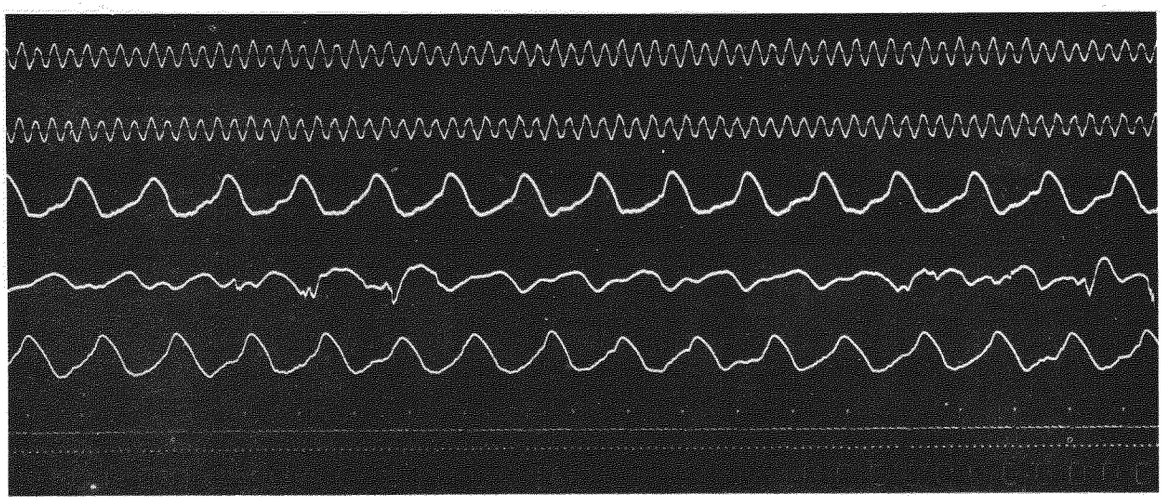

C5/105 $V_A/U = 0{\cdot}302$

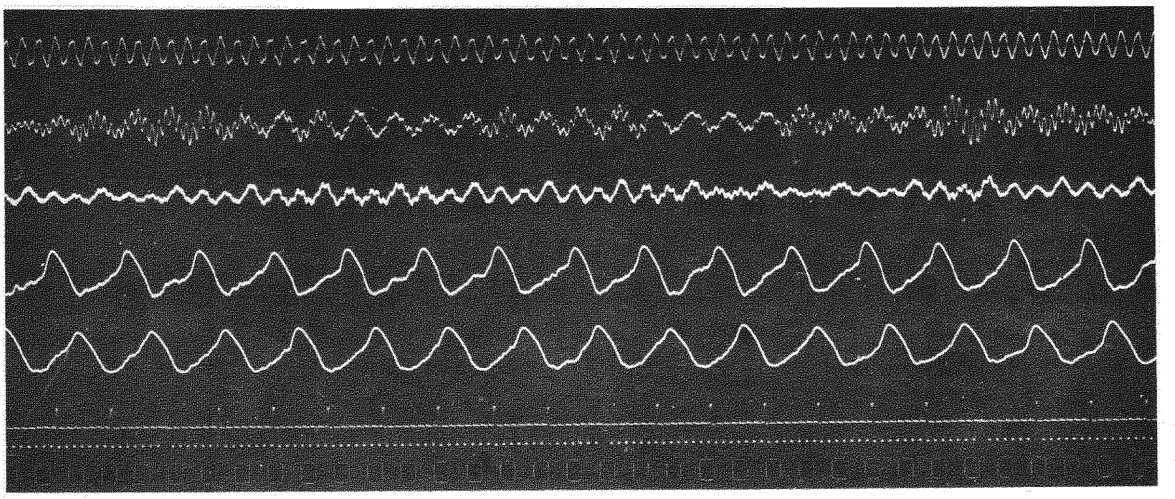

C5/104 $V_A/U = 0{\cdot}302$

RECORDS AT 5000 R.P.M.

FIG. 15

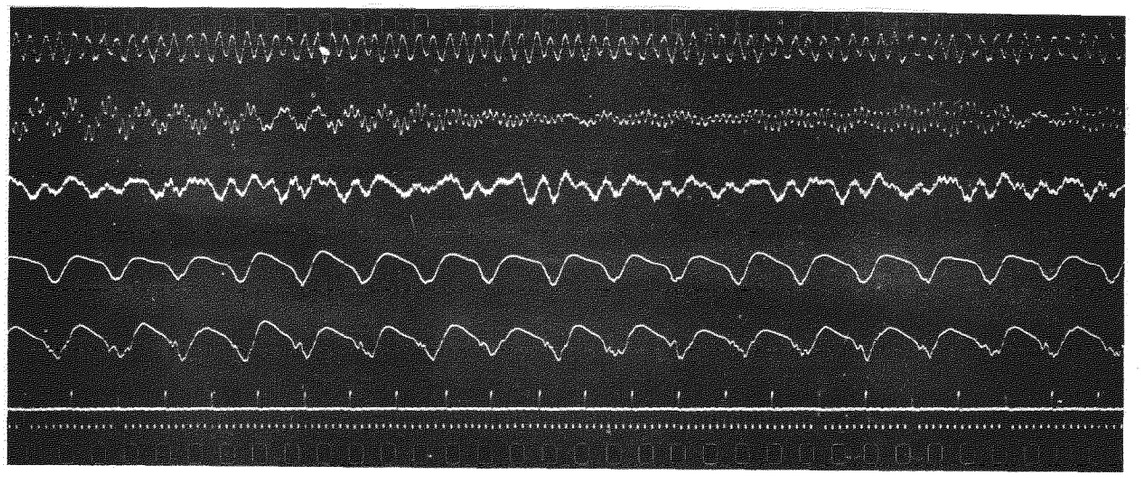

D4/145 $V_A/U = 0.432$

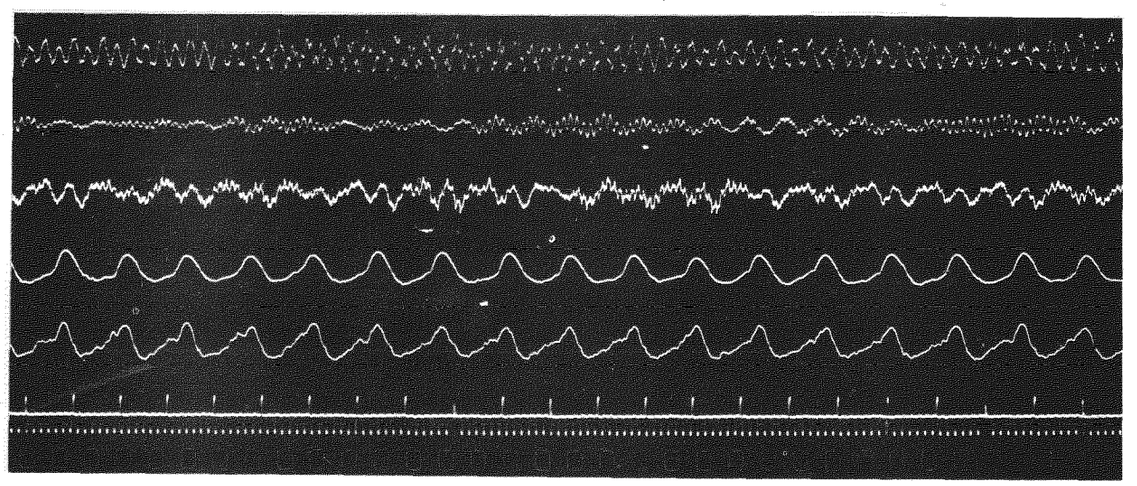

D5/154 $V_A/U = 0.293$

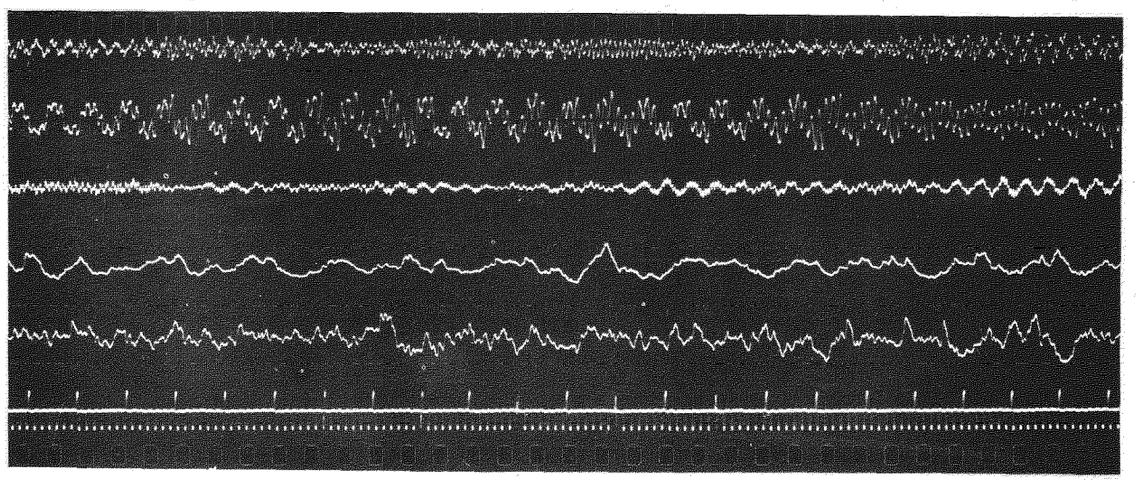

D6/161 $V_A/U = 0.184$

RECORDS AT 5500 R.P.M.

FIG. 16

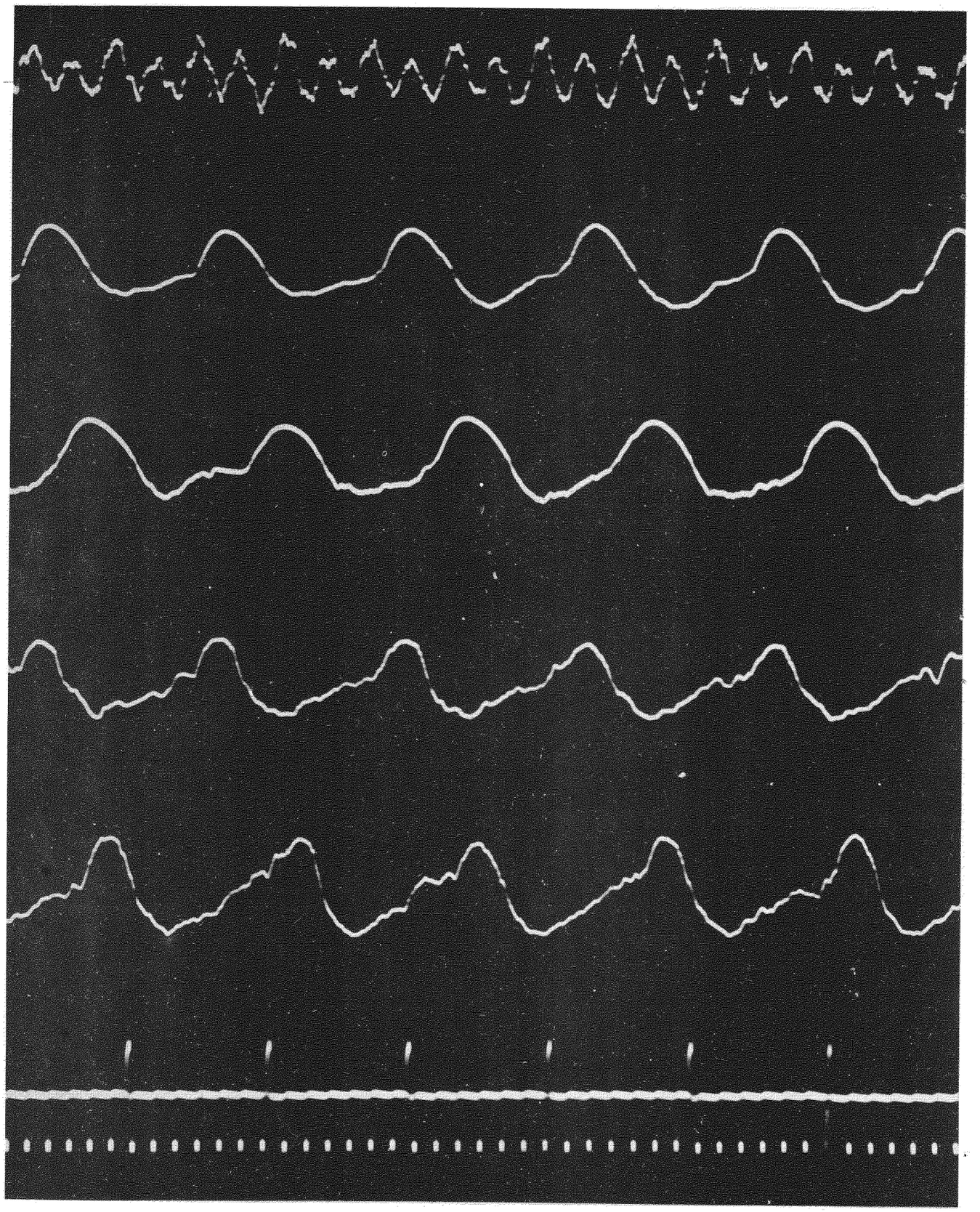

D5/150

$V_A/U = 0.293$

STALL CELLS IN INLET
GUIDE AND STATOR ROWS 5500 R.P.M.

FIG. 17

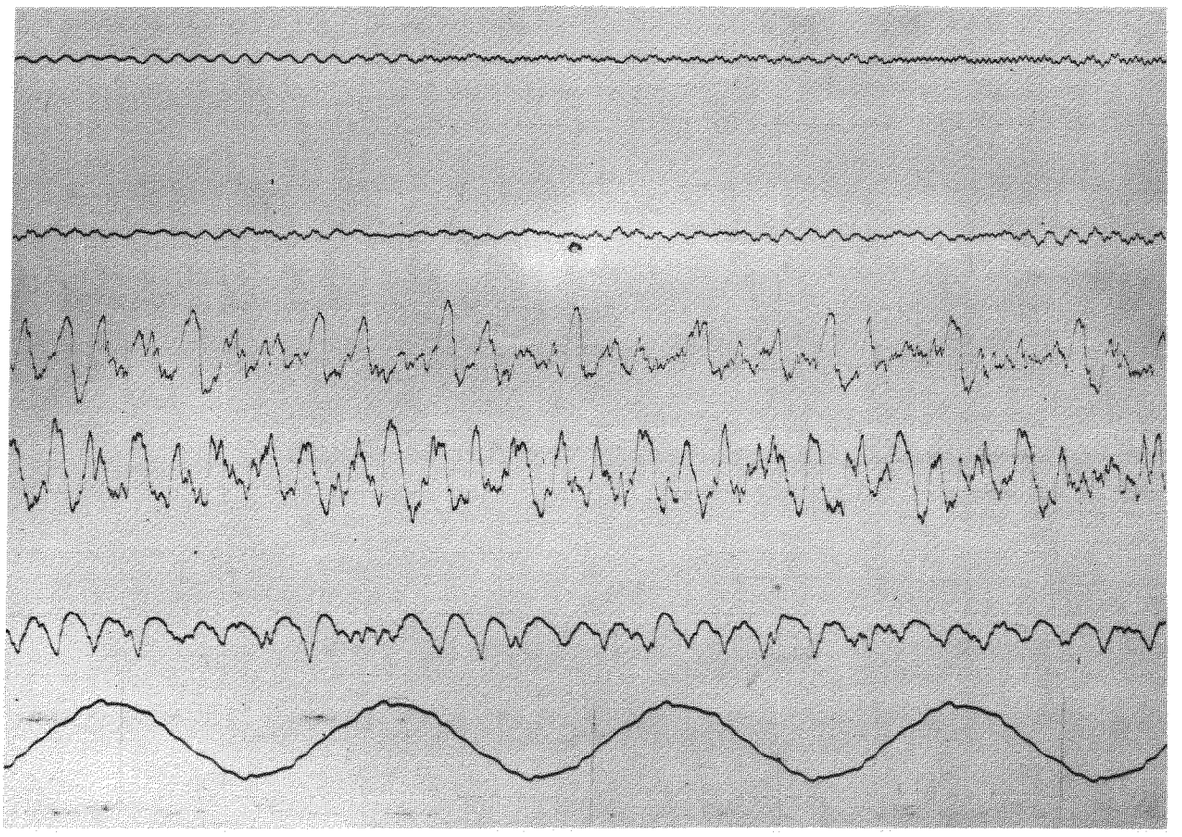

REC. 9 $V_A/U = 0 \cdot 285$ 4000 R.P.M.

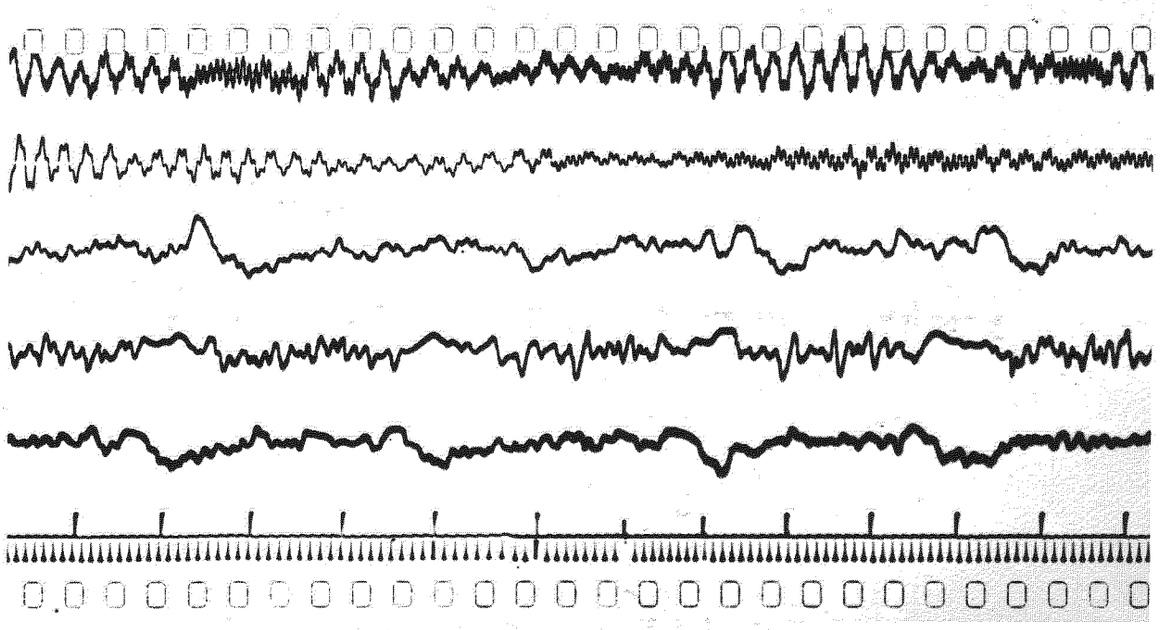

A5/28 $V_A/U = 0 \cdot 295$ 4000 R.P.M.

COMPARABLE
SINGLE AND MULTISTAGE RECORDS

FIG. 18

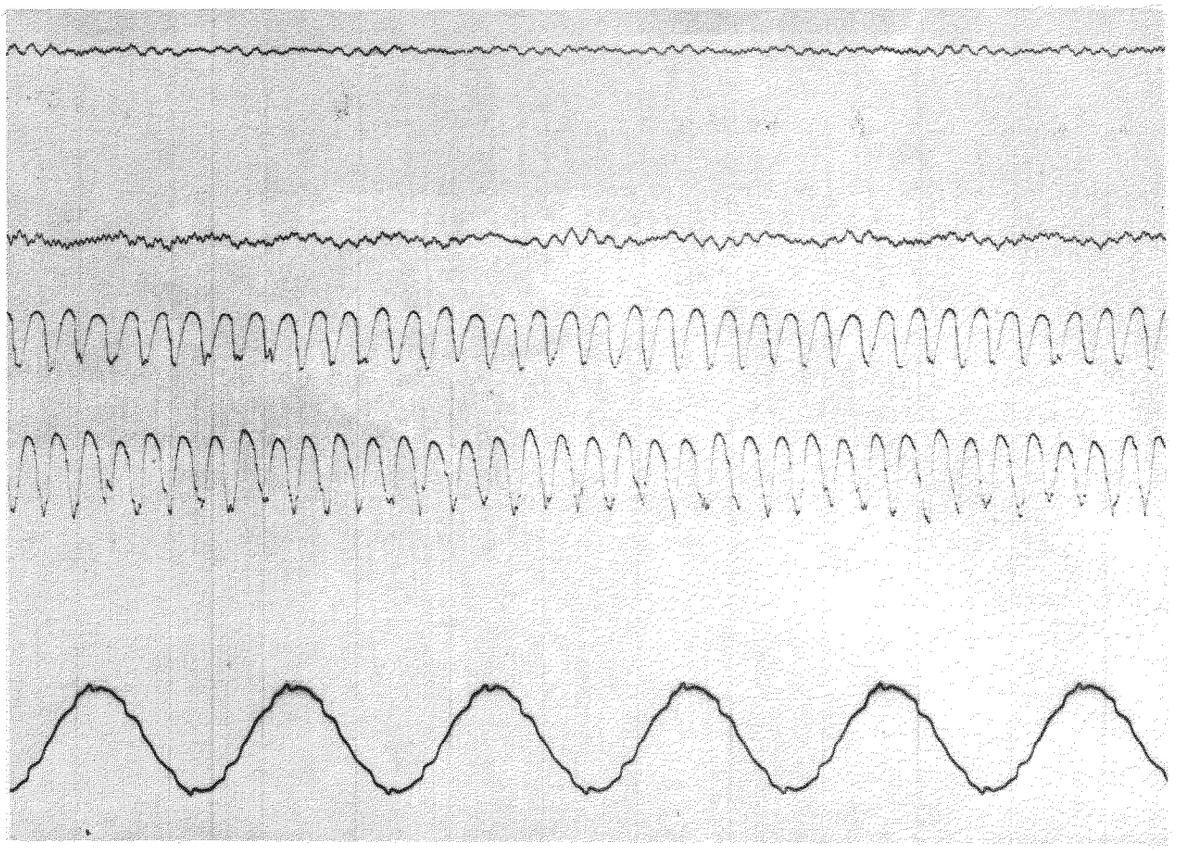

REC. 37 $V_A/U = 0.31$ 5700 R.P.M.

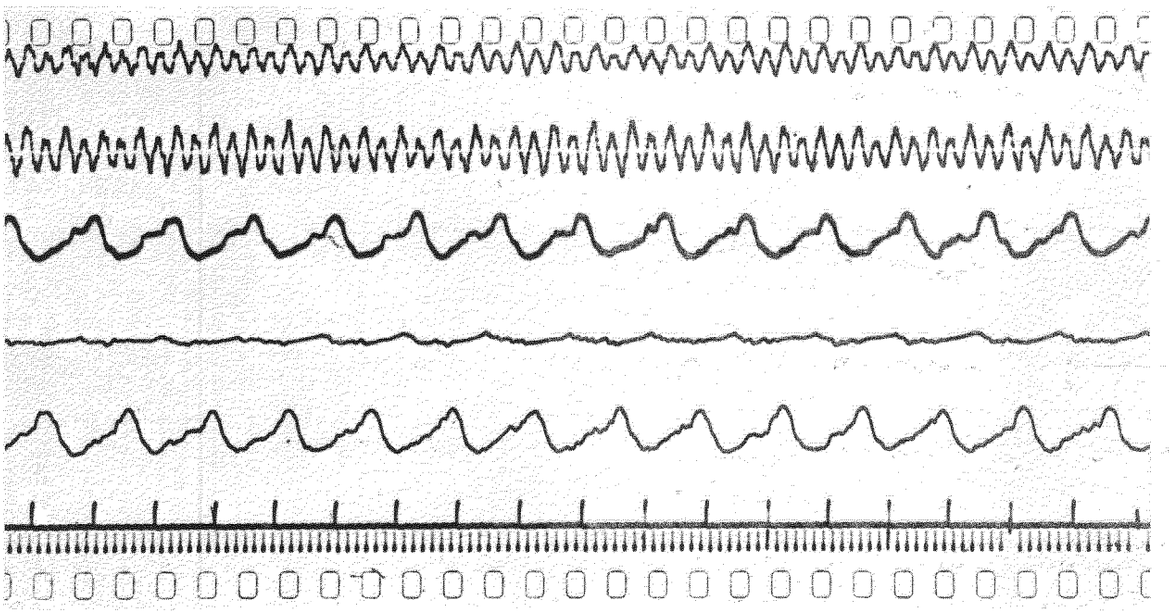

D5/151 $V_A/U = 0.295$ 5500 R.P.M.

COMPARABLE SINGLE AND MULTISTAGE RECORDS

DS88195/1 W160 KA 3/61 R&CL

C.P. No. 537
April, 1958
Chaplin R.

621.438.031.3-226.2:
539.3:621.004.63

FLOW FLUCTUATIONS AND ALTERNATING BLADE STRESSES IN A SINGLE-STAGE COMPRESSOR; A COMPARISON WITH MULTI-STAGE TESTS

A single-stage compressor was assembled to be identical with the first stage of a multi-stage compressor. The fluctuations in axial velocity and the alternating stresses in the blades were measured and are compared with those which existed in the multi-stage compressor at identical speeds and non-dimensional flows.

No similarity was observed in the number, size or speed of rotation of the stall cells and it is concluded that measurements of alternating stress in a single-stage compressor are not necessarily a guide to those in the same stage when forming part of a multi-stage compressor.

The alternating blade stresses have been calculated from the observed fluctuations in velocity and a reasonable agreement between measured and calculated values obtained.

C.P. No. 537
April, 1958
Chaplin R.

621.438.031.3-226.2:
539.3:621.004.63

FLOW FLUCTUATIONS AND ALTERNATING BLADE STRESSES IN A SINGLE-STAGE COMPRESSOR; A COMPARISON WITH MULTI-STAGE TESTS

A single-stage compressor was assembled to be identical with the first stage of a multi-stage compressor. The fluctuations in axial velocity and the alternating stresses in the blades were measured and are compared with those which existed in the multi-stage compressor at identical speeds and non-dimensional flows.

No similarity was observed in the number, size or speed of rotation of the stall cells and it is concluded that measurements of alternating stress in a single-stage compressor are not necessarily a guide to those in the same stage when forming part of a multi-stage compressor.

The alternating blade stresses have been calculated from the observed fluctuations in velocity and a reasonable agreement between measured and calculated values obtained.

C.P. No. 537
April, 1958
Chaplin R.

621.438.031.3-226.2:
539.3:621.004.63

FLOW FLUCTUATIONS AND ALTERNATING BLADE STRESSES IN A SINGLE-STAGE COMPRESSOR; A COMPARISON WITH MULTI-STAGE TESTS

A single-stage compressor was assembled to be identical with the first stage of a multi-stage compressor. The fluctuations in axial velocity and the alternating stresses in the blades were measured and are compared with those which existed in the multi-stage compressor at identical speeds and non-dimensional flows.

No similarity was observed in the number, size or speed of rotation of the stall cells and it is concluded that measurements of alternating stress in a single-stage compressor are not necessarily a guide to those in the same stage when forming part of a multi-stage compressor.

The alternating blade stresses have been calculated from the observed fluctuations in velocity and a reasonable agreement between measured and calculated values obtained.

Printed and published by
HER MAJESTY'S STATIONERY OFFICE

To be purchased from
York House, Kingsway, London W.C.2
423 Oxford Street, London W.1
13A Castle Street, Edinburgh 2
109 St. Mary Street, Cardiff
39 King Street, Manchester 2
50 Fairfax Street, Bristol 1
2 Edmund Street, Birmingham 3
80 Chichester Street, Belfast 1
or through any bookseller

Printed in England

S.O. Code No. 23-5012-37